AN ABSTRACT OF THE THESIS OF

ROBERT JAMES LILLIE for the degree of MASTER OF SCIENCE

in Geophysics presented on FEBRUARY 4, 1977

Title: SUBSURFACE GEOLOGIC STRUCTURE OF THE VALE, OREGON, KNOWN GEOTHERMAL RESOURCE AREA FROM THE INTERPRETATION OF SEISMIC REFLECTION AND POTENTIAL FIELD DATA

Abstract approved: Redacted for privacy

Dr. Richard W. Couch

Seismic reflection, gravity, and magnetic data, collected in 1974 and 1975 by personnel from Oregon State University, the University of Oregon, and Portland State University, and integrated with existing surface geologic and well log data, show major subsurface structural features in the Vale Known Geothermal Resource Area in eastern Oregon. Computation of the depth to magnetic basement shows that the magnetic source is less than 30 meters below the surface in an area 20 kilometers south of Vale, Oregon, where beds of the Grassy Mountain Basalt are exposed. In an area of Cow Hollow, south of Vale, covered by sediments of the Chalk Butte Formation, the top of the magnetic basement is estimated to be at least 150 meters below the surface. A two-dimensional crustal model across Double Mountain in T.20S., R.44E., constrained by total field magnetic data, suggests that truncated edges of uplifted basalt flows can account for observed high frequency magnetic anomalies.

Data from four split-spread seismic reflection lines in the Cow Hollow and Sand Hollow areas south and southwest

of Vale show interval velocities from 1.9 to 3.4 km/sec, characteristic of sedimentary sequences, and higher velocity intervals from 3.4 to 7.0 km/sec, suggesting sequences of basalt and intercalated sediments. These, along with published surface geologic and well log data, provide constraints for two-dimensional crustal sections constructed to agree with observed free-air gravity anomalies. The sections show that a major structural feature, interpreted as a horst block, extends southward from Vale Buttes to the Owyhee Reservoir. High Bouguer gravity anomaly gradients, trending north-south south of Vale and northeast-southwest along the Owyhee River, delineate bounding faults on the horst.

Free-air and complete Bouguer gravity anomaly maps and a map of the second derivative of gravity in the area between latitudes 43°15' and 44°15' North and longitudes 117°00' and 118°00' West show other tectonic features in the Vale-Owyhee region. A high gravity gradient following Willow Creek northwest of Vale and extending into Idaho near Nyssa, Oregon, suggests a major northwest-southeast trending structure. Other published data suggest that this feature may be a right-lateral strike-slip fault terminating the northern end of the Basin and Range Province. Other high Bouguer gravity anomaly gradients suggest normal faults striking N 20°W in the area north of the Bully Creek Reservoir, northwest of Vale. These proposed faults show bending or offset to a north-south trend south of the reservoir. High Bouguer gravity anomaly values northeast of Vale suggest that the Snake River Basin has been filled with high density material.

Mapped thermal springs and wells in the Vale-Owyhee region generally occur on or near proposed major faults. This suggests that the faults serve as zones of high permeability for the flow of deep thermal waters to the surface.

Subsurface Geologic Structure of the Vale, Oregon, Known Geothermal Resource Area from the Interpretation of Seismic Reflection and Potential Field Data

by

Robert James Lillie

A THESIS

submitted to

Oregon State University

in partial fulfillment of
the requirements for the
degree of

Master of Science

Completion 4 February 1977

Commencement June 1977

APPROVED:

Redacted for privacy

Associate Professor of Geophysics
in charge of major

Redacted for privacy

Dean of the School of Oceanography

Redacted for privacy

Dean of Graduate School

Date thesis is presented FEBRUARY 4, 1977

Typed by Deanna L. Cramer for Robert James Lillie

ACKNOWLEDGEMENTS

Dr. Richard Couch served as my major professor. I am grateful to him for his enlightening suggestions and strong encouragement in the preparation of this thesis.

I appreciate the helpful comments from Drs. Gunnar Bodvarsson and Robert Lawrence on my thesis area.

Steve Pitts deserves special thanks for his unceasing (and almost insane) determination to keep the computer software, so vital to this thesis, going.

I would like to thank the members of the geophysics field crew -- Rick Blakely, Jeb Bowers, Bart Brown, Gerry Connard, Jan Donovan, Dwight Eggers, Tom Flaherty, Bill French, Ansel Johnson, Paul Jones, Ken Keeling, Judy Keser, Walt Lynn, Rick McAlister, Mike Moran, Gordon Ness, Tom Plawman, Linda Victor, and Steve Woodcock -- without whose assistance I would have had no data to work with. Most especially, I would like to thank Kevin Larsen for the two hot summers he spent in the field in eastern Oregon collecting gravity data.

The people who drafted the illustrations -- Jan Gemperle, Jack Weissman, Tracy Colby, Barbara Priest, and Virginia Taylor -- were very kind, considering all the trouble I gave them. Judy Brenneman showed what a fine person she is by typing the rough draft of this thesis. Deanna Cramer did an excellent job of typing the final copy.

I would like to give special thanks to my office mates -- Shane Coperude, John Norton, and Tom Plawman -- without whose timely humor I would not have been able to keep my sanity in the preparation of this thesis.

Very special thanks go to Marie-Annick, who did not consider it too much trouble to fly across an ocean to help me keep my spirits up.

My parents deserve an immeasurable amount of thanks for their help and encouragement during my years in school.

This research, initiated under the auspices of the Oregon State Department of Geology and Mineral Industries, was funded by U.S. Geological Survey Grants 14-08-0001-G-222 and 14-08-0001-G-230.

TABLE OF CONTENTS

LIST OF TABLES

LIST OF FIGURES

List of Figures (continued)

SUBSURFACE GEOLOGIC STRUCTURE OF THE VALE, OREGON, KNOWN GEOTHERMAL RESOURCE AREA FROM THE INTERPRETATION OF SEISMIC REFLECTION AND POTENTIAL FIELD DATA

INTRODUCTION

The Vale Hot Spring area in east central Oregon (see location map, figure 1) is thought to possess substantial geothermal resource potential. Roy, et al. (1971) show the area to lie within a zone of high heat flux roughly following the North American Cordillera. Bowen (1972) and Hull (1975) reported borehole temperature gradients as high as 153.8°C/km in the vicinity of Vale. This compares with a normal gradient of about 30°C/km for continental areas (Garland, 1971). Bowen and Peterson (1970) show evidence of surface and near surface thermal activity in the form of thermal springs and shallow hot water wells. Van Orstrand (1935) reported surface temperatures as high as 94.2°C in flowing wells at Vale.

Physical criteria outlined in the Geothermal Steam Act of 1970 (Godwin, et al., 1971) resulted in the designation of the Vale Hot Spring area as a Known Geothermal Resource Area (KGRA). This means the area's geothermal resource potential is thought valuable enough to warrent expenditures of money for geothermal exploration. Factors considered in assigning the KGRA status to an area include the presence of late Tertiary or Quaternary volcanics as well as the thermal phenomena mentioned above. Studies by both public and private groups to better define and develop the geothermal resource potential of the Vale area are presently in progress.

In September, 1974 personnel from the Geophysics Group of Oregon State University, the Department of Earth Sciences of Portland State University, and the Department of Geology

Washington

1 Mount St. Helens

Oregon

1 Breitenbush Hot Springs
2 Crump Geyser
3 Vale Hot Springs
4 Mount Hood
5 Lakeview
6 Carey Hot Springs
7 Klamath Falls

Idaho

1 Yellowstone
2 Frazier

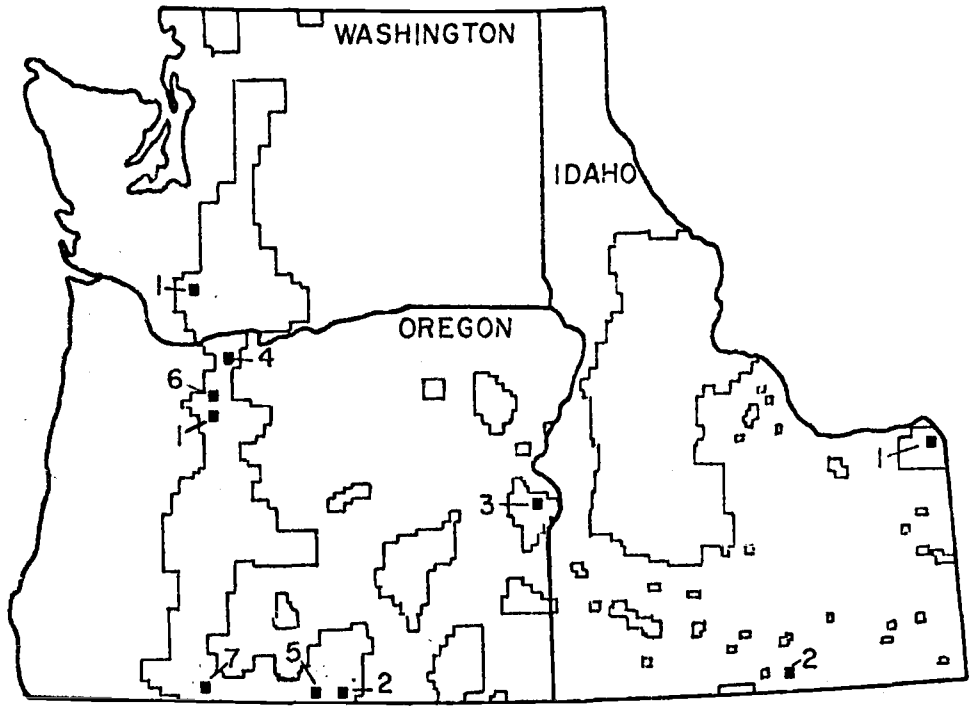

Figure 1. Index map of Oregon, Washington, and Idaho showing lands classified for geothermal resources effective December 24, 1970 (from Godwin, et al., 1971).

of the University of Oregon began the collection of geophysical data from the Cow Hollow and Sand Hollow areas southwest of Vale. Couch, et al. (1975) give details of the objectives of this work. Data collected include the four split-spread seismic reflection lines and the four total field magnetic profiles shown in figure 2. Larson and Couch (1975) discuss later field work consisting of 812 gravity measurements in the area between latitudes 43°15' and 44°15' North and longitudes 117°00' and 118°00' West.

The present study is a reduction and interpretation of the geophysical data obtained in the studies mentioned above. Published surface geology and well log data provide further information for the interpretation of subsurface structure in the area.

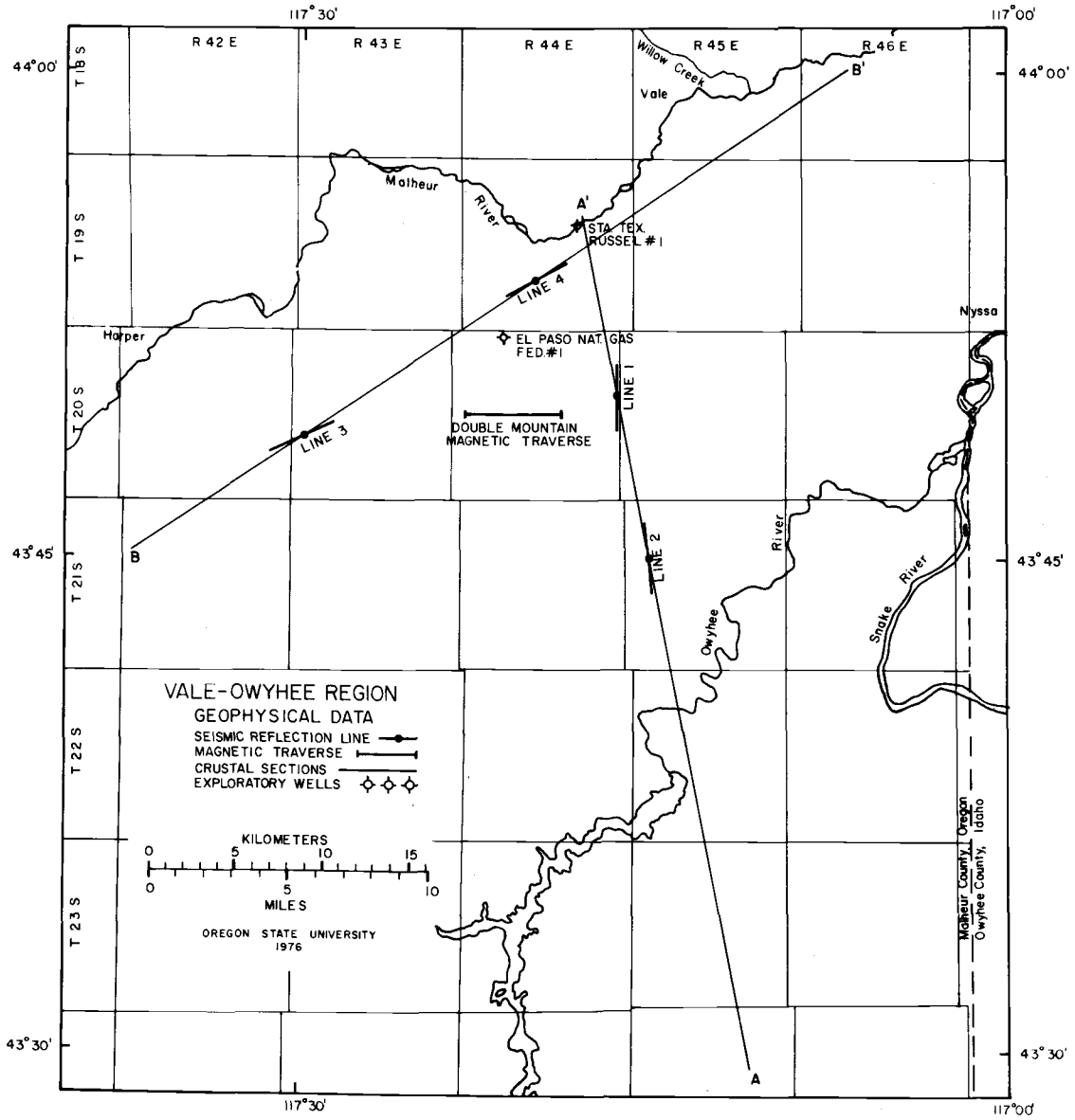

Figure 2. Index map showing location of crustal cross sections constructed using geophysical data in the Vale area.

GEOLOGIC SETTING

General Geology

Studies of the Mitchell Butte Quadrangle by Corcoran, et al. (1962) and the Owyhee Region by Kittleman, et al. (1965, 1967, 1973) provide descriptions and maps of the surface geology of areas surrounding the Vale Hot Springs Known Geothermal Resource Area. Newton and Corcoran (1963) reported subsurface conditions observed in exploratory oil and gas wells in the area. Below is a brief summary of these studies.

Physiographically, the Vale KGRA lies near the juncture of the Columbia Plateau Province and the Basin and Range Province. The major tectonic feature of the area is the Snake River Downwarp, extending from the area of Yellowstone Park, through the present Snake River Valley and into east-central Oregon. The western part of this downwarp is known as the Snake River Basin. Deposition of thousands of meters of interbedded volcanics and sediments of fluvial and lacustrian origin occurred here in Miocene and Pliocene time.

Topographic highs in the area are generally resistant basalt flows while softer sedimentary deposits form low areas. Igneous intrusives of both basic and acidic nature are found throughout the stratigraphic sequence. These form positive topographic expressions, generally in the form of domes.

Faults south of Vale generally trend north-south, possibly showing the northernmost extent of the Basin and Range Province. Faults trend in a more northwesterly direction north of Vale. Regional dip in the area is northeasterly, toward the axis of the Snake River Basin.

Stratigraphy

The uppermost unit in the stratigraphic sequence is the Idaho Group of lower to middle Pliocene age, named by Cope (1883). Corcoran, et al. (1962) later divided this group into three formations. The upper Pliocene Chalk Butte Formation consists of loosely consolidated, tuffaceous sandstones, siltstones, and conglomerates deposited in fluviatile and lacustrian environments. Minor amounts of tuff, ashbeds, fresh water limestones and thin basalt flows are also present. Because of the soft nature of these rocks, the Chalk Butte Formation generally crops out as low rounded hills.

Underlying the Chalk Butte Formation is the middle to lower Pliocene Grassy Mountain Basalt, first named by Bryan (1929). This formation consists of massive basalt flows up to 40 meters thick with interbedded sediments. Newton and Corcoran (1963) describe cuttings from the El Paso Natural Gas Company, Federal No. 1 well in sec. 5, T. 20S., R. 44E. which indicate the total thickness of the formation may be 350 meters or more. Due to its resistant nature, the Grassy Mountain Basalt caps many ridges in the mapped areas.

The lowermost formation of the Idaho Group is the Kern Basin Formation of early Pliocene age. It consists of up to at least 250 meters of tuff, tuffaceous silstone, low rank graywacke, and occasional conglomerates. A few thin basalt flows and sills are also present.

Lying unconformably below the beds of the Idaho Group is the Deer Butte Formation of late Miocene age. The basal part of the formation is made up of fine-grained tuffaceous sediments with a few interbedded basalt flows. These grade upward into massive well cemented sandstones and conglomerates. Corcoran, et al. (1962) believe the Mascall

Formation of central Oregon correlates stratigraphically with the Deer Butte Formation. The maximum measured thickness of the formation is about 400 meters.

Another large unconformity occurs between the Deer Butte Formation and the underlying Owyhee Basalt, first named by Bryan (1929). The Owyhee Basalt is also of late Miocene age and probably correlates with the Columbia River Basalt of north central Oregon. The sequence consists of very dense to highly vesicular flows with interbedded tuff and ash deposits. Maximum thickness is at least 500 meters at surface exposures fringing the Snake River Basin.

The oldest beds exposed on the western fringe of the basin belong to the Sucker Creek Formation of Miocene age. The formation consists mainly of altered tuffs, volcanic and arkosic sandstones, tuffaceous shales, and siltstones. A series of basaltic lava flows appears near the base of the sequence and rhyolites occur in the upper part. The maximum exposed thickness of the formation is about 700 meters.

Numerous igneous intrusives of widely differing ages cut the stratigraphic sequence. These are generally in the form of feeder dikes or large domes. These rocks range from rhyolites and dacites to basalts and gabbros. The Double Mountain anticline in T. 20 and 21 S., R. 44 E. is a large scale example of one of the many intrusives.

GEOPHYSICAL DATA

Field Techniques

Figure 3 shows the location of the seismic reflection and magnetic lines. The four split-spread seismic reflection lines were each approximately 4000 meters (13,000 feet) long and consisted of 36 geophone groups at spacings of 107 meters (350 feet). Charges were 2 to 100 pounds of Tovex detonated in 9 meter (30 foot) cased drill holes. A seismic field truck recorded events in analog form on magnetic tape. The truck's playback system also served to filter unwanted high and low frequency events from the seismic reflection records (Couch, et al., 1975).

Total magnetic field measurements made using a proton precession magnetometer were spaced at 30 to 100 meter (100 to 300 foot) intervals. Three of the survey lines follow reflection lines 1, 2, and 3, while the fourth is a 4-1/2 kilometer (3 mile) east-west traverse across Double Mountain.

Figure 4 (Couch and Baker, 1977) shows the locations of gravity stations in the area between latitudes 43°15' and 44°15' North and longitudes 117° and 118° West used in this study. Kevin Larson made 812 of these measurements during the summers of 1974 and 1975 with Wordon Gravity Meter 575. Larson and Couch (1975) discussed aquisition and preliminary analysis of this data. Additional measurements reported by Thiruvathukal, et al. (1970) provide additional data. All of these measurements are relative to a base station at the Ontario, Oregon, airport established by Berg and Thiruvathukal (1965) which has a reported value of 980,304.19 ± .08 mgal. Preliminary reduction of these data reported by Couch and Baker (1977) yielded the free-

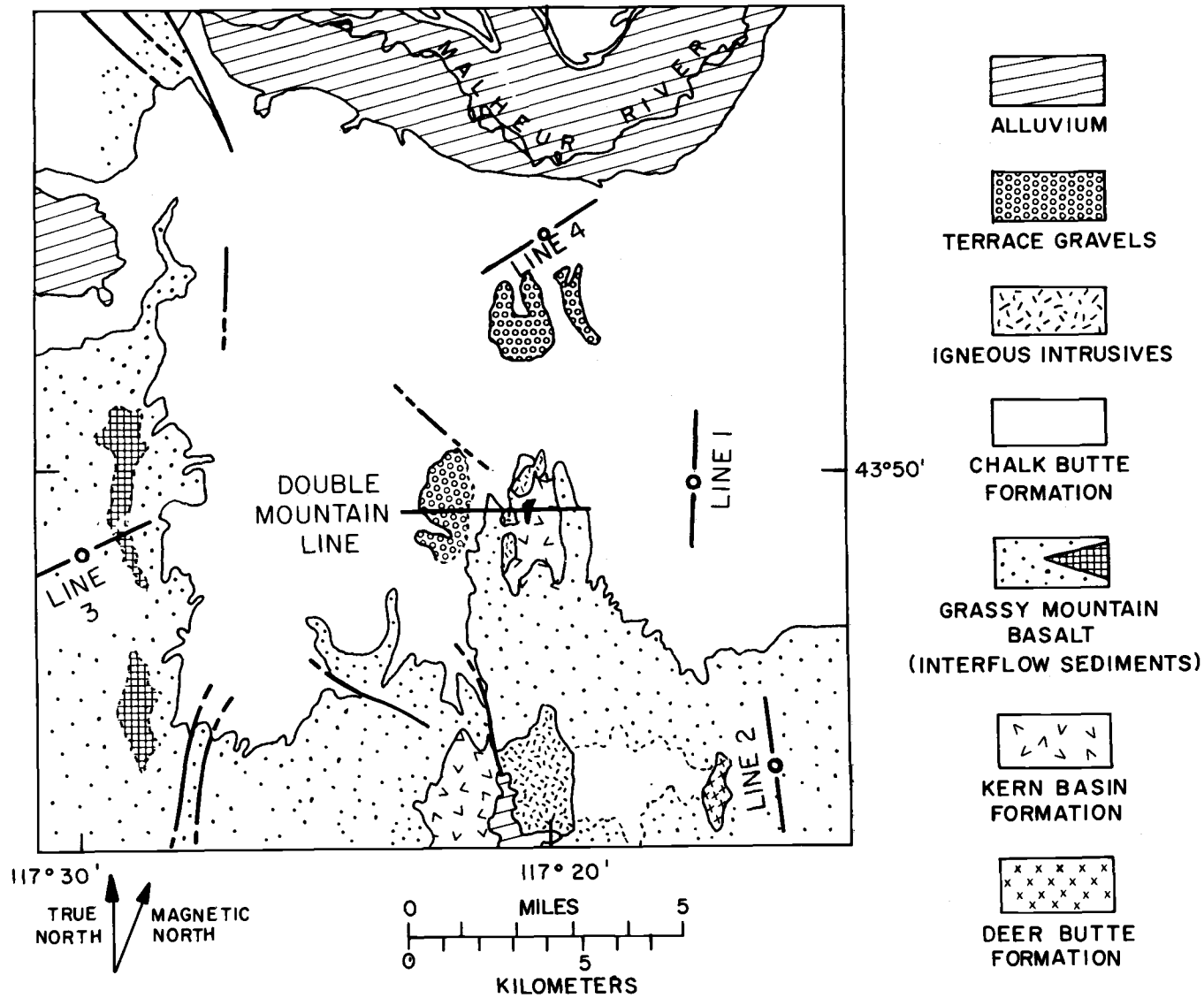

Figure 3. Location of seismic reflection and magnetic lines in the Cow Hollow and Sand Hollow areas southwest of Vale. Surface geology from Corcoran, et al. (1962).

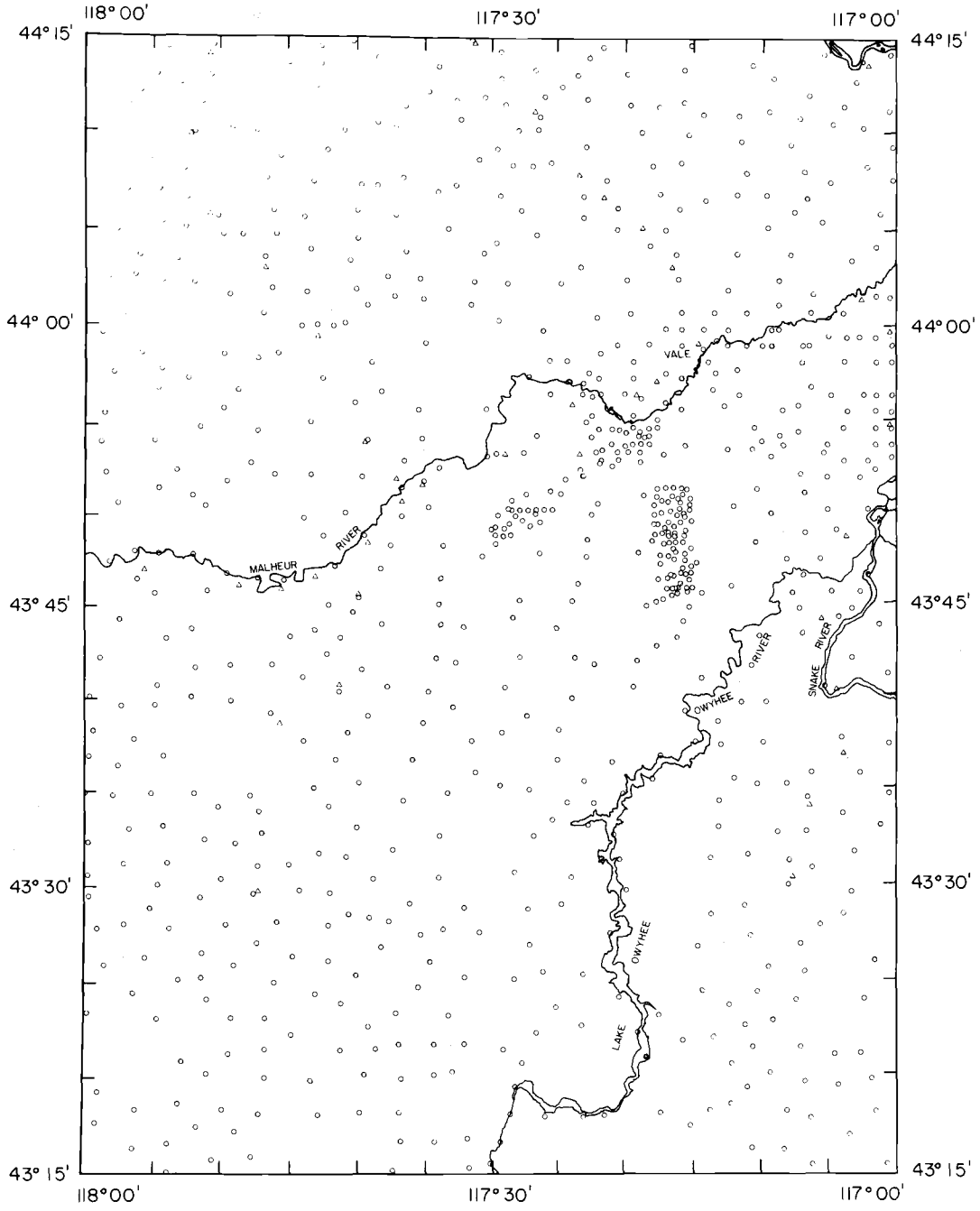

GRAVITY STATIONS

VALE-OWYHEE REGION, MALHEUR COUNTY, OREGON

AREA OF THIS MAP

KILOMETERS

0 5 10 15 20 25 30 35

0 5 10 15 20

MILES

TRANSVERSE MERCATOR PROJECTION

GRAVITY STATIONS

△ J. THIRUVATHUKAL 1969 OSU

○ K. LARSEN 1974 – 1975 UO

OREGON STATE UNIVERSITY

SEPTEMBER, 1976

Figure 4. Location of gravity stations in the Vale-Owyhee region (from Couch and Baker, 1977).

air and complete Bouguer anomaly maps shown in figures 5 and 6.

Reduction and Interpretation

Magnetic Data

Figure 7 shows profiles of magnetic data along seismic reflection lines 1, 2, and 3. A regional average of 55,700 gammas subtracted from observed values gives the total field magnetic anomalies. Analysis of these data provides estimates of depth to magnetic basement along the reflection lines.

Anomalies associated with lines 2 and 3 are of high amplitude (approximately 1000 gammas) and short wavelength (approximately 60 meters). This suggests the magnetic basement is at a shallow depth along these lines. The half-slope method discussed by Peters (1949), applied to a typical anomaly on line 2, suggests the magnetic source is only 27 meters below the surface on that line. Surface lithology, such as flows of the Grassy Mountain Basalt which crops out along the length of lines 2 and 3, also suggests a shallow source.

The profile of line 1, however, shows anomalies of relatively low amplitude (approximately 160 gammas) and long wavelength (approximately 1000 meters). This line rests upon sediments of the Chalk Butte Formation. Presumably, anomalies caused by a source (i.e. basalt) buried by the sediment are geometrically attenuated (i.e. anomalies are low because the source is some distance below the observation points).

Upward continuation techniques such as those described by Schouten and McCamy (1972) provide a means by which magnetic profiles measured at different levels above magnetic sources can be compared. Figure 8 shows the results of

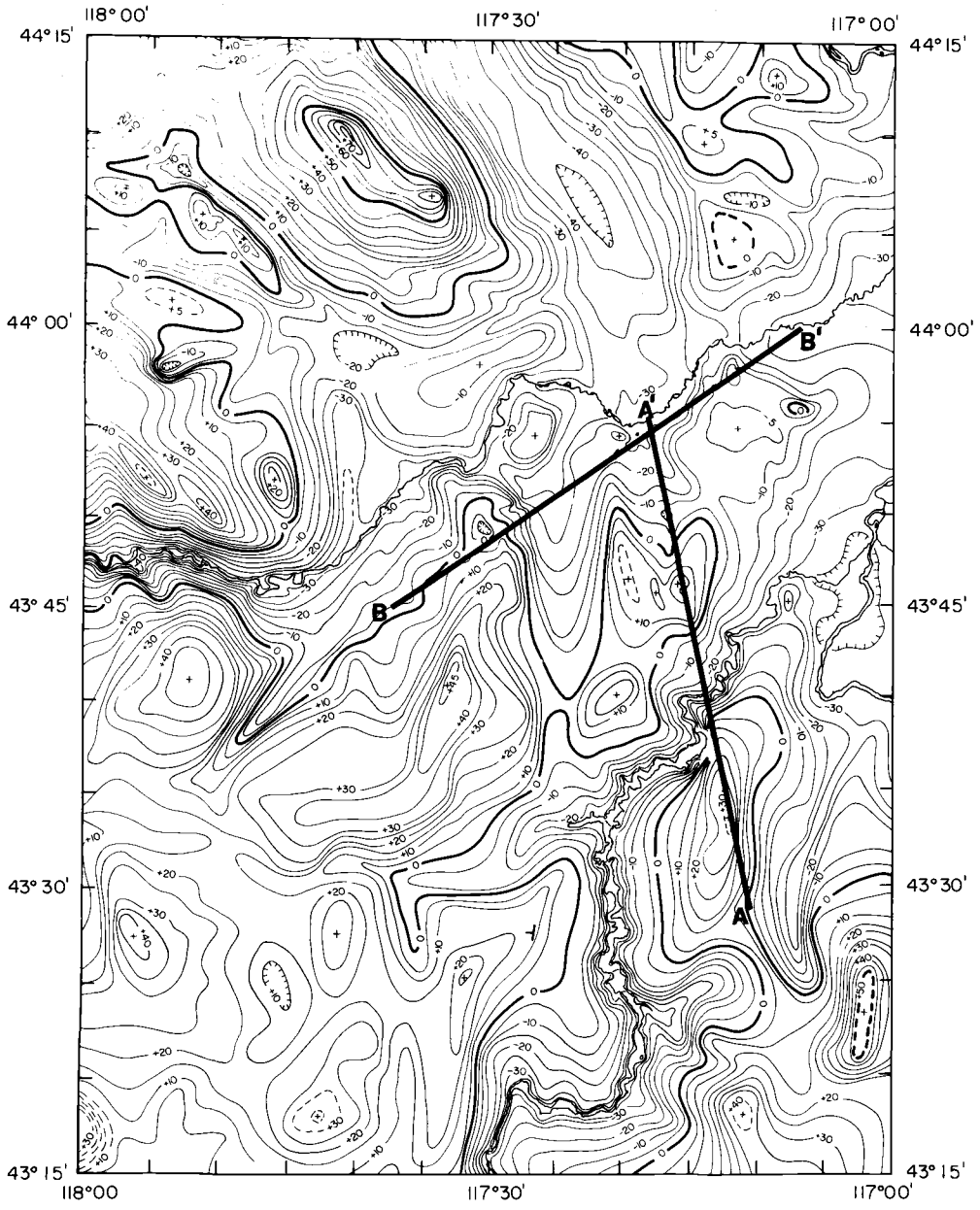

FREE-AIR GRAVITY MAP

VALE-OWYHEE REGION, MALHEUR COUNTY, OREGON

AREA OF THIS MAP

KILOMETERS 0 5 10 15 20 25 30 35

MILES 0 5 10 15 20

CONTOUR INTERVAL 5.0 MGALS

ESTIMATED STATION UNCERTAINTY ± 1MGAL

GRAVITY DATA FROM

J. THIRUVATHUKAL 1969 OSU

K. LARSEN 1975 UO

OREGON STATE UNIVERSITY

SEPTEMBER, 1976

Figure 5. Free-air gravity anomaly map of the Vale-Owyhee region with location of crustal sections A-A' and B-B'.

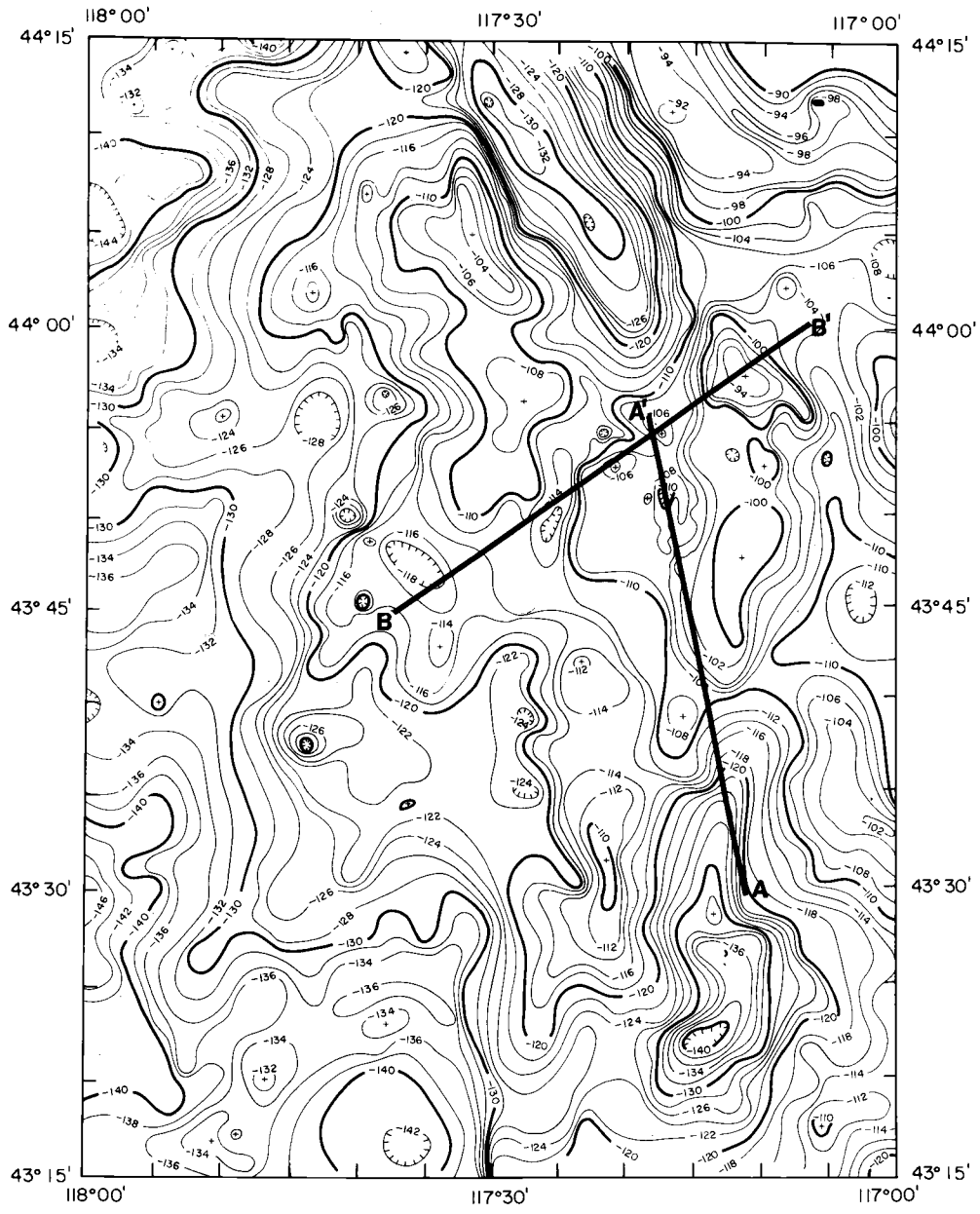

Figure 6. Complete Bouguer gravity anomaly map of the Vale-Owyhee region. The assumed Bouguer reduction density is 2.67 gm/cm^3.

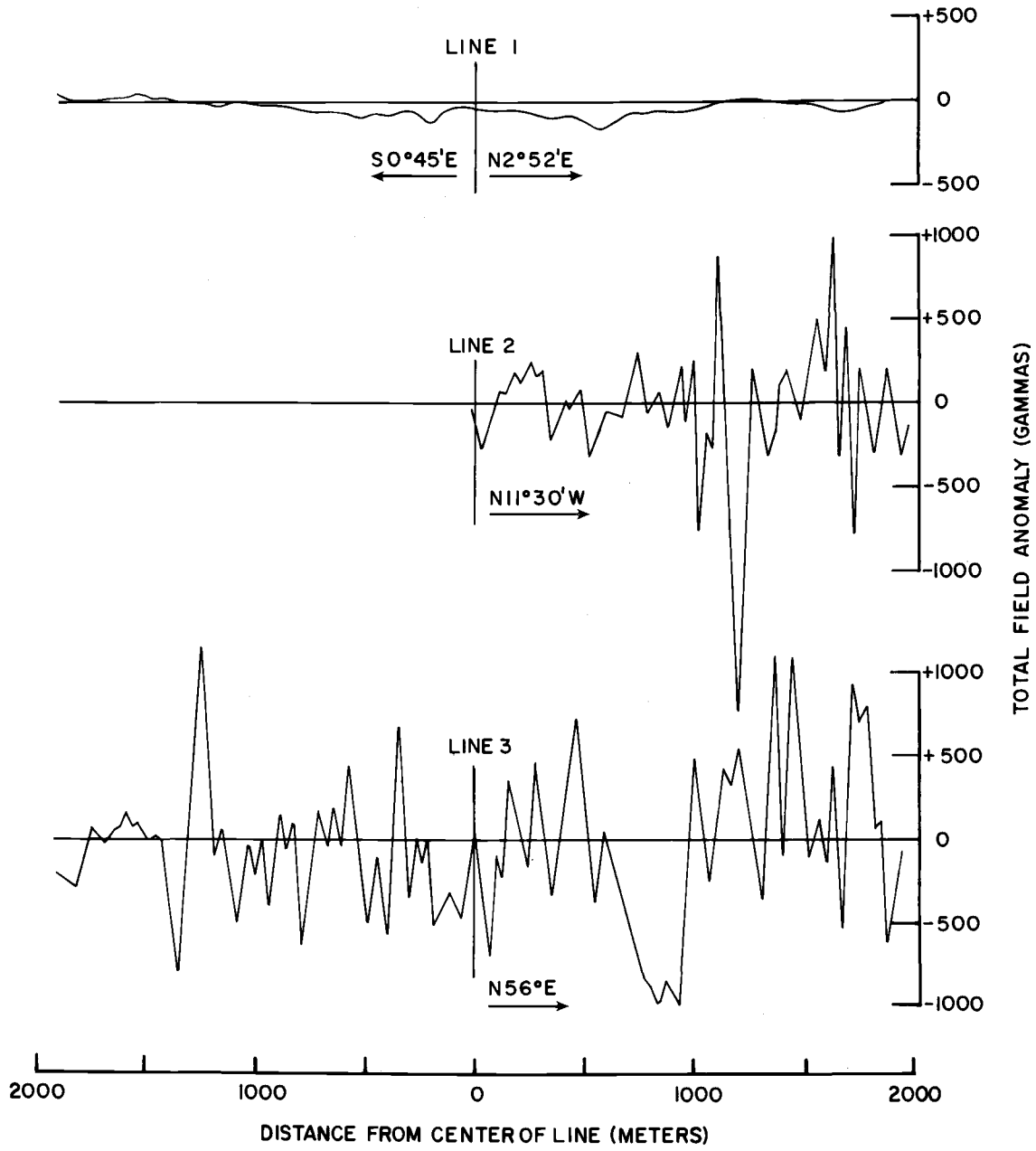

Figure 7. Magnetic profiles 1, 2, and 3. A regional average of 55, 700 gammas is subtracted from observed values to produce the total field anomaly.

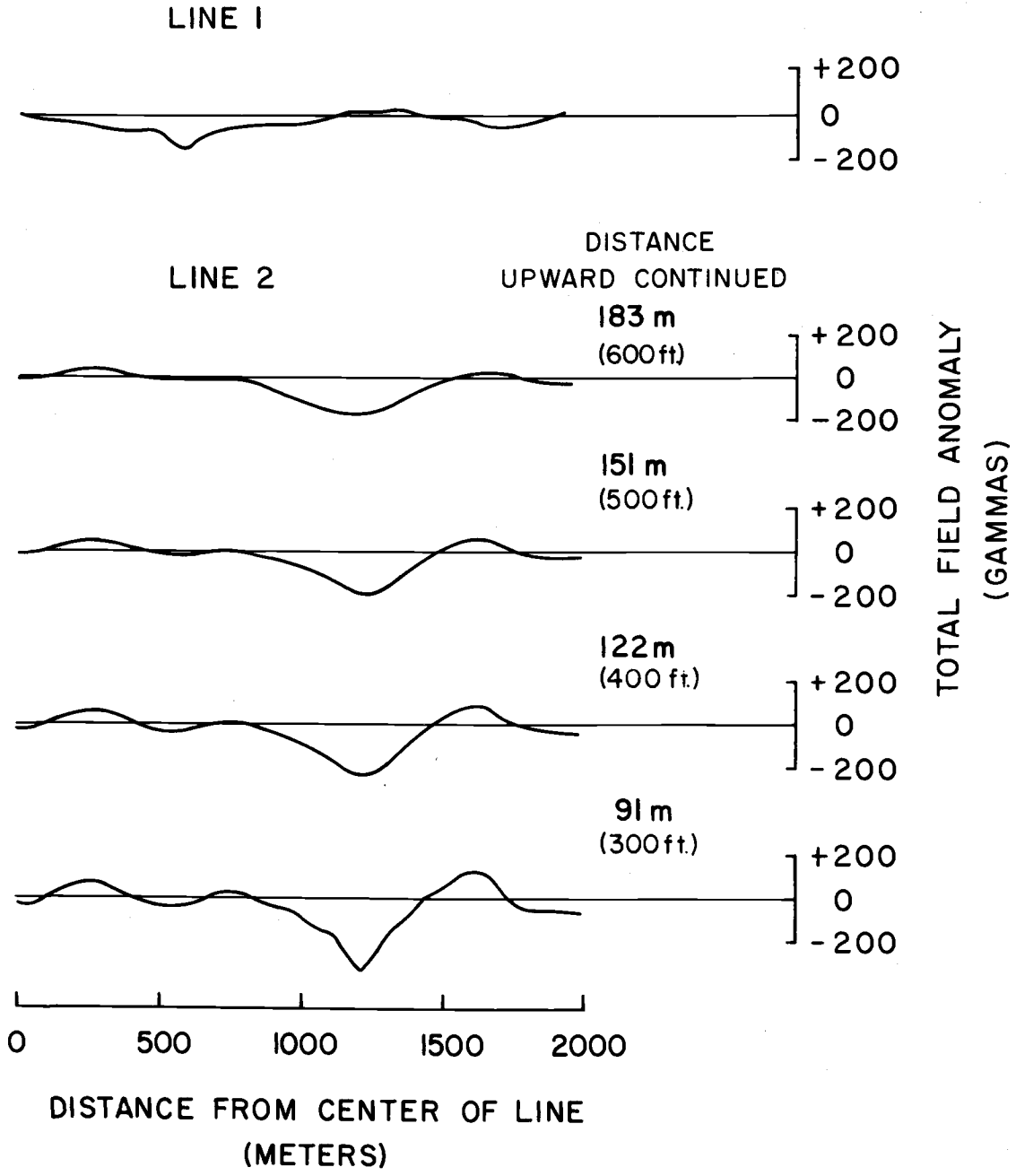

Figure 8. Upward continuation of magnetic profile 2 with the north part of magnetic profile 1 for comparison.

upward continuation of line 2 along with the north side of line 1 for comparison. The profiles should look similar in wavelength and amplitude when measured at the same distance above the source. This similarity begins to appear between the 151 and 183 meter upward continuation profiles. These distances provide an estimate of the minimum depth to magnetic basement along line 1. In conclusion, a basaltic magnetic source occurs near or at the surface on lines 2 and 3 while at least 151 meters (500 feet) of sediment is estimated to overlie the basalt on line 1.

The Double Mountain traverse crosses an anticlinal uplift mapped as a dacite intrusion by Corcoran, et al. (1962). Interbedded basalts and sediments of the Kern Basin Formation, Grassy Mountain Basalt, and Chalk Butte Formation, cut by the intrusion, crop out away from the dacite core.

Talwani and Heirtzler (1964) formulated a method to calculate the total magnetic field across a two-dimensional earth model. In their method, a postulated model consists of uniformly magnetized blocks of earth material assumed infinite in a direction perpendicular to the direction of the magnetic profile. All magnetization is assumed induced by the earth's field (i.e. remnant magnetization is considered zero). Blakely (1975) incorporated the technique of Talwani and Heirtzler in a computer program to calculate magnetic anomalies due to a two dimensional earth model. This program was used to calculate total field anomalies for hypothetical magnetic models of Double Mountain.

Figure 9 shows a proposed two-dimensional model of Double Mountain. The Double Mountain anticline south of Vale, Oregon, trends approximately north-south and the magnetic traverse is oriented approximately east-west, normal to the axis of the anticline. The two-dimensional assumption, therefore, is considered valid for an approximation of the near-surface structure. The value of magnetic

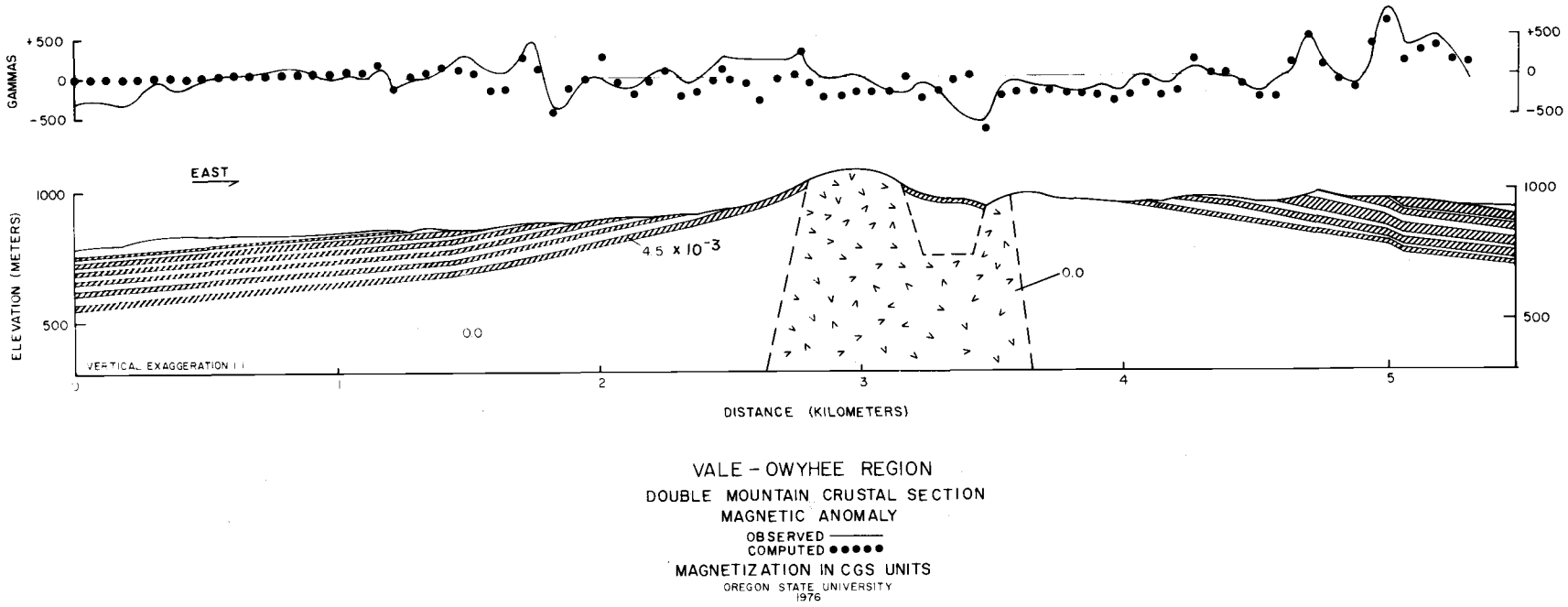

Figure 9. Double Mountain crustal section. Basalt flows are shown by the striped pattern, dacite by the "v" pattern, and sedimentary layers are left blank.

susceptibility selected for basalt in this study is in the upper part of the range of values listed by Grant and West (1965) for basic effusive rocks. Because typical values for sediments and dacite are very small, the susceptibilities of these rocks are considered zero in the model.

The solid line above the Double Mountain model in figure 9 is a plot of the observed total magnetic field with a regional average of 55,700 gammas removed. Dots represent magnetic anomalies calculated assuming the proposed model. The observed field shows wavelengths as small as 300 meters and peak-to-peak amplitudes as high as 1500 gammas. The model shows that truncated edges of basalt flows at or near the surface can cause these anomalies.

Seismic Reflection Data

Variations in the acoustic properties of subsurface geologic materials cause the reflection and refraction of seismic waves. Arrivals of energy following reflected and refracted paths are recognized after filtering unwanted signals such as low frequency surface waves from seismic reflection records and are interpreted in terms of geologic structure.

Arrivals of compressional waves following direct and critically refracted paths provide information on near surface layers below reflection lines 1, 2, 3, and 4. The recursive relations of Adachi (1954), modified to fit split-spread data and applied to seismic waves detected along the reflection lines, give the seismic velocities shown in Table 1. On lines 1 and 4, layer 1 is estimated to have a seismic velocity between 1.98 and 2.12 km/sec. This is a typical velocity for poorly lithified sediments. These two lines are located on sediments of the Chalk Butte Formation. Material with a velocity of 3.86 to 4.32 km/sec occurs immediately below this layer on lines 1 and 4 and

Table 1. Layer velocities and thicknesses from refraction events on seismic reflection records.

Layer		Velocity (km/sec)	Thickness (meters)
Line 1	1	1.98	166
	2	4.16	
Line 2	2	4.32	
Line 3	2	4.06	
Line 4	1	2.12	241
	2	3.86	

at the surface on lines 2 and 3. These higher velocities likely are associated with basalt flows in the Grassy Mountain Basalt which crop out on lines 2 and 3. The 166 meters of sediment overlying the basalt on line 1 is in agreement with the thickness of sediment determined from the magnetic data.

Reflection events from nearly horizontal interfaces approximate hyperbolas on reflection records. Grant and West (1965) describe techniques by which average seismic velocities and thicknesses of earth materials below seismic lines are estimated from reflection hyperbolas. Table 2 shows estimates of average velocities and thicknesses of intervals of earth material below reflection lines 1, 2, 3 and 4, computed using the T^2-X^2 method. Reflection hyperbolas chosen for this analysis are correlatable between reflection records. The interval velocities computed represent the average velocity of earth material between

Table 2. Layer velocities and thicknesses from T^2-X^2 analysis of seismic reflection records.

Interval		Velocity (km/sec)	Thickness (meters)
Line 1	I	1.97	171
	II	4.18	752
	III	2.86?	749?
	IV	9.01?	1230?
Line 2	II	4.05	454
	III	2.92	668
	IV	7.68?	1517?
Line 3	II	3.42	639
	III	2.78?	463?
	IV	6.54?	1293?
Line 4	I	1.98	204
	II	3.66	818
	III	3.43	568
	IV	6.18?	1312?

reflecting interfaces. These interval velocities also correlate from shotpoint to shotpoint.

The 200 meters of low velocity material (interval I) on lines 1 and 4 are the sediments observed from the refraction and magnetic analysis. Likewise, higher velocity material (interval II) occurs below this and at the surface on lines 2 and 3. Estimated maximum thickness of this interval is 818 meters, as calculated for line 4 using the T^2-X^2 method. An interval of lower velocity material occurs below this on each of the lines (interval III), underlain by material of higher velocity (interval IV).

It is emphasized that the velocities calculated are interval velocities and are therefore an average for a large thickness of material. Intervals with velocities characteristic of sediment may also contain thin basalt interbeds. These basalts presumably have velocities much higher than the surrounding sediments. The entire interval, however, will show an average velocity close to that of sediment. Likewise, intervals consisting predominately of basalt with interbedded sediments will have a velocity characteristic of basalt when large thicknesses are considered. It is also emphasized that this is a seismic section. An attempt is made below to correlate calculated seismic velocity intervals with geologic formations observed at the surface. Reflection horizons chosen for the velocity analysis, however, are arbitrary and do not necessarily lie at the contact between geologic formations. The correlations, therefore, are between seismic velocity intervals observed from the reflection records, and stratigraphic sequences from surface geology and well log data.

Table 3 shows a suggested relation between the calculated seismic intervals and the stratigraphic sequence of Corcoran, et al. (1962) for the Mitchell Butte quadrangle. These correlations, along with well log descriptions from Newton and Corcoran (1963), provide additional constraints for crustal cross sections constructed in agreement with gravity observations discussed below.

Gravity Data

Preliminary reduction of the observed gravity data by Kevin Larson and Steve Pitts of the University of Oregon (Couch and Baker, 1977) yielded free-air and complete Bouguer gravity anomaly maps. The International Gravity Formula $TG = 978049.0\ (1 + 0.0052884\ \sin^2\theta - 0.000059\ \sin^2 2\theta)$mgals, where θ is the latitude, gives the theoretical

Table 3. Seismic velocity intervals, suggested lithology, and suggested correlation with stratigraphic sequence of Corcoran, et al. (1962).

Interval	Approximate Velocity (km/sec)	Approximate Thickness (meters)	Suggested Lithology	Suggested Stratigraphic Correlation
I	1.9-2.1	At least 240	Loosely consolidated sediment	Chalk Butte Fm.
II	3.4-4.2	500-800	Basalt with interflow sediments	Grassy Mountain Basalt
III	2.7-3.4?	450-750?	Sediment with intercalated basalt	Kern Basin Fm. Deer Butte Fm.
IV	6.2-9.0?	1200-1500?	Basalt with rhyolite and sediments	Owyhee Basalt Part of Sucker Creek Fm.

gravity for each of the stations in the study area. The formula FA = (OG + 0.3086h) - TG, where OG is the observed gravity and h is elevation in meters above sea level, gives free-air anomaly values used in the contour map of figure 5. Simple Bouguer anomalies result from the formula SB = FA - 0.012774 ρh where ρ is the reduction density, selected to be 2.67 gm/cm^3 in the reduction by Larson and Pitts. Terrain corrections applied to the simple Bouguer anomalies give the complete Bouguer gravity anomalies used to construct the contour map of figure 6 (Couch and Baker, 1977).

In addition to these standard types of gravity anomaly maps, a map of the second derivative of the complete Bouguer anomalies is included in this study. In order to reduce edge effects, this analysis included additional gravity values from areas fringing the Vale-Owyhee region. Thiruvathukal et al. (1970) give 153 gravity measurements in the zone within 30 minutes of longitude and latitude of the study area on the Oregon side. A study by Baldwin and Hill (1960) includes 209 values between 116°30' and 117°00' West longitude in Idaho adjacent to the Vale-Owyhee region. Henderson and Zietz (1949) present a technique by which second derivatives may be computed from an evenly spaced grid of gravity values. An evenly spaced grid with a 3.2 kilometer spacing between grid points was constructed by interpolating between contours of the complete Bouguer gravity anomaly map of figure 10. Constants chosen for the second derivative analysis are based on the assumption that the maximum radius of Bouguer gravity anomalies is about 25 kilometers.

The estimated average density of crustal rocks penetrated by the El Paso Natural Gas, Federal Spurier #1 well, obtained using a technique discussed below, is 2.404 gm/cm^3. Therefore, in order to minimize topographic effects, complete Bouguer values computed assuming a reduction density of 2.4 gm/cm^3 are used in the second derivative analysis.

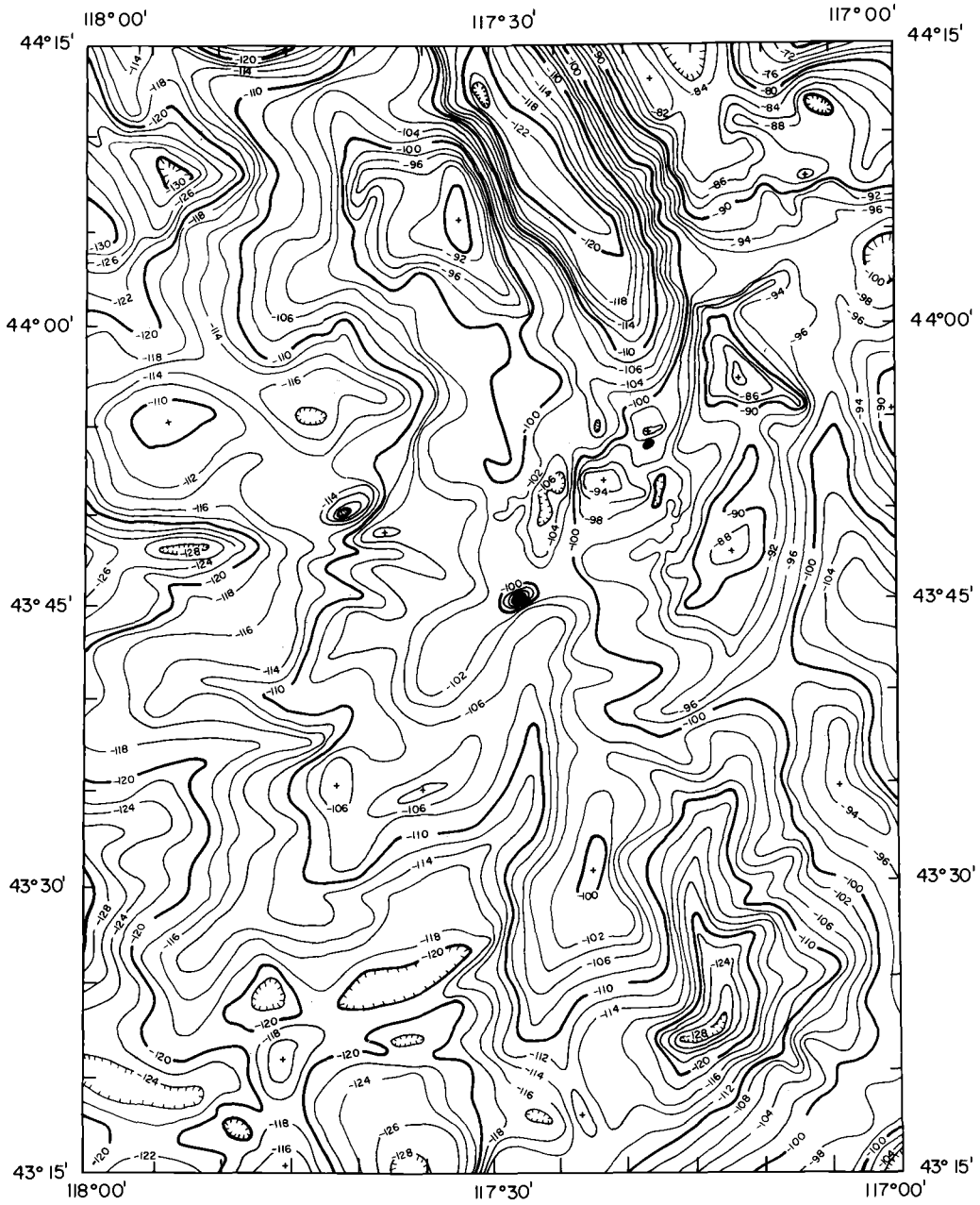

COMPLETE BOUGUER GRAVITY MAP

VALE-OWYHEE REGION, MALHEUR COUNTY, OREGON

AREA OF THIS MAP

KILOMETERS 0 5 10 15 20 25 30 35

MILES 0 5 10 15 20

CONTOUR INTERVAL 2.0 MGALS
ESTIMATED STATION UNCERTAINTY ± 1 MGAL
REDUCTION DENSITY 2.40 gm/cm^3

GRAVITY DATA FROM
J THIRUVATHUKAL 1969 OSU
K LARSEN 1975 UO

OREGON STATE UNIVERSITY
DECEMBER, 1976

Figure 10. Complete Bouguer gravity anomaly map of the Vale-Owyhee region. The assumed Bouguer reduction density is 2.40 gm/cm^3.

Figure 11 is the resulting contour map of the second derivative of gravity in the Vale-Owyhee region. A discussion of features observed on this and the other gravity maps follows.

The formula to compute the free-air anomaly, FA = (OG + 0.3086h) - TG, discussed earlier, corrects for contributions to the acceleration of gravity due to rotation of the earth and variation of the radius to the center of the earth due to latitude and elevation. The free-air gravity anomaly map of the Vale-Owyhee region (figure 5) is a function of total mass below the area. Variations in the densities of rocks below the surface or uncompensated topography may account for the anomalies. Therefore, the free-air anomaly map is influenced by both topography and deep structural features.

The free-air anomalies of the Vale-Owyhee region correlate, in part, with topography. Large anomaly lows parallel the canyons of the Owyhee River in the southeast and the Malheur River in the western part of the map. Highs generally correlate with mountainous areas such as Juniper Mountain in the northeast part of the map and Owyhee Ridge, just east of the Owyhee Reservoir. Overall trends in the area apparently show surface expressions of the juncture between Basin and Range topography to the south and the Snake River Basin to the north. Anomalies on the southern part of the map trend north-south while a northwesterly trend is seen north of Vale. The gravity anomaly trends follow both topography and fault trends as mapped by Corcoran, et al. (1962) and Kittleman, et al. (1967).

A broad free-air anomaly low extends southeastward from latitude 44°15' North, longitude 117°30' West to the Malheur River near Vale, Oregon. The course of Willow Creek follows the high gravity gradient on the northeast side of the anomaly. The closure of 20 mgals on this

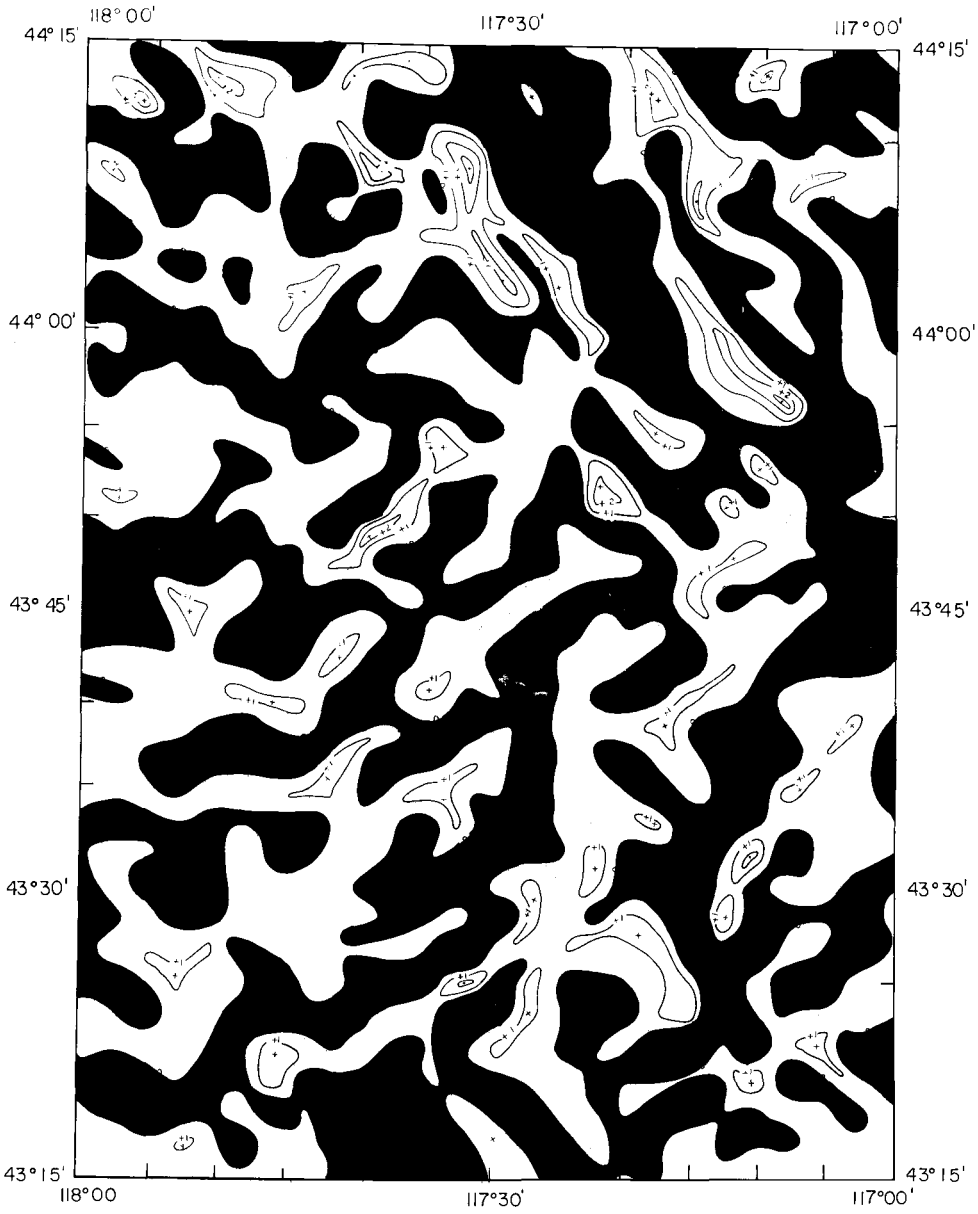

SECOND DERIVATIVE OF COMPLETE BOUGUER GRAVITY

VALE-OWYHEE REGION, MALHEUR COUNTY, OREGON

AREA OF THIS MAP

KILOMETERS

0 5 10 15 20 25 30 35

0 5 10 15 20

MILES

CONTOUR INTERVAL 1.0 mgals/km^2

BOUGUER REDUCTION DENSITY 2.40 gm/cm^3

GRAVITY DATA FROM

J.THIRUVATHUKAL 1969 OSU

K.LARSEN 1975 UO

OREGON STATE UNIVERSITY

DECEMBER, 1976

Figure 11. Second derivative map of complete Bouguer gravity anomalies in the Vale-Owyhee region. The assumed Bouguer reduction density is 2.40 gm/cm^3. Areas of negative second derivative values are shaded while positive areas are left blank.

anomaly low suggests mass deficiency below the surface. Structural implications of the feature are discussed later in this thesis.

The simple Bouguer anomaly correction subtracts the gravity effect due to mass between the observation point and a sea level datum. Additionally, effects due to curvature of the earth and mass above (e.g. mountains) or lack of mass below (e.g. canyons) the observation point, known collectively as terrain corrections, are removed to produce the complete Bouguer anomaly. An approximate average density must be assigned to masses subtracted or added, therefore the resulting anomaly map is a function of the reduction density chosen. Because material above sea level is obviously not homogeneous in density, the Bouguer correction does not entirely remove topographic effects in all parts of the map. The complete Bouguer anomaly map shows evidence of deep structure by minimizing effects due to topography.

A standard reduction density of 2.67 gm/cm^3 was used in constructing the map of figure 6. Topographic effects due to features such as the Owyhee River canyon are still evident, but greatly reduced. Bouguer anomalies trend north-south below latitude 44°00' North and northwest-southeast north of 44° North latitude. This suggests that deep structural trends are similar to near surface trends shown by topography, major faults, and free-air gravity anomalies.

Two large gravity anomalies of interest occur in the mapped area. The first is the elongate low mentioned above extending about 35 kilometers in a northwesterly direction from Vale to the northern edge of the map at latitude 44°15' North. The amplitude of the complete Bouguer anomaly is about 12 mgals. The northeast side of this low roughly follows the course of Willow Creek. Topographic relief in the Willow Creek valley, however, is not nearly enough to

account for the amplitude of the observed gravity anomaly. The low Bouguer gravity anomaly values, like the free-air gravity anomaly values, indicate a mass deficiency below the surface.

Bowen and Blackwell (1975) propose one explanation for the structure of the Willow Creek Valley. They postulate a downdropped block bounded by faults on either side of the valley. Their conclusions are based on a limited amount of gravity and magnetic measurements as well as the physiographic expression of the area. They also postulate that high heat flow and geothermal manifestations in the form of Vale Hot Springs and several warm water wells reflect leakage along a southwest dipping fault parallel to and just to the west of Willow Creek. The gravity low seen on the complete Bouguer anomaly map could be due to the accumulation of low density sediments in the proposed graben structure. Evidence of throw along proposed faults from surface geology or well data, however, is lacking at this time.

The second large Bouguer anomaly of interest is on the eastern part of the map, extending southward for 40 kilometers from just east of Vale to the Owyhee River. The amplitude of the Bouguer gravity high is about 10 mgals. Topographic highs along the anomaly include the Vale Buttes to the north and Mitchell Butte to the south. While topography may in part cause the anomaly, it is estimated from modeling (discussed below) that the amplitude of the anomaly is primarily due to mass excess below the surface. The anomaly follows a north-south trend of inliers of the Deer Butte Formation mapped by Corcoran, et al. (1962). The gravity anomaly thus suggests a structural trend between these isolated topographic features.

The gravity high lies very near the area of detailed seismic reflection work described above. Subsurface structure below the area of the gravity anomaly is therefore estimated by extrapolation of the seismic control data in

agreement with the measured gravity data. This structural interpretation is included in the following discussion of two model crustal sections.

Figure 2 shows the locations of the two crustal sections constrained by the observed free-air gravity values. Interpolation between observed gravity measurements is on the basis of contours from the free-air gravity anomaly map. Section A-A' runs N 12°W, passing through seismic reflection shot points 1 and 2 and crossing section B-B' very near Sta Tex Oil Company, R.A. Stamey, Russel #1 well in sec. 14, T. 19S, R. 44E. Shot points 3 and 4 lie along section B-B' while El Paso Natural Gas, Federal Spurier #1 well in sec. 5, T. 20S, R. 44E is within 2 kilometers of the line. Data from the reflection spreads and well log descriptions, along with mapped surface geology, provide constraints for the crustal sections.

Local changes of the earth's gravity field are due, in part, to variations in the density of near-surface crustal layers. Seismic velocity intervals and lithologic descriptions from well logs provide means to estimate average densities of intervals of earth materials. Ludwig, Nafe, and Drake (1971) present a plot of seismic velocity versus density for typical rocks. Table 4 gives estimates of average densities of the seismic intervals discussed above,

Table 4. Estimated average densities of seismic velocity intervals.

Interval	Approximate Velocity (km/sec)	Approximate Density from Nafe-Drake Curves (gm/cm^3)
I	1.9-2.1	1.9-2.1
II	3.4-4.2	2.3-2.5
III	2.7-3.4?	2.2-2.3?
IV	6.2-9.0?	2.5-3.7?

based on the Nafe-Drake curves. Newton and Corcoran (1963) give lithologic descriptions of drill cuttings from the two wells mentioned above. The sequences consist of volcanic sediments interspersed with basaltic to rhyolitic extrusive rocks. Thick intervals consisting entirely of sediments can be distinguished from intervals consisting of alternating sedimentary and volcanic rocks. Dobrin (1960) gives average densities for these rock types. The average density of an interval is thus estimated from the drill cutting descriptions by weighting densities according to lithology and depth of burial. Table 5 shows the results of this analysis along with a suggested correlation of the intervals chosen from the well logs with the seismic velocity intervals.

Talwani, et al. (1959) present a method to compute the total vertical gravitational attraction across a two-dimensional earth model. The model consists of homogeneous blocks of earth material assumed infinite in a direction perpendicular to the orientation of the crustal section. Gemperle (1975) incorporated similar methods in a computer program used to compute free-air anomalies in this thesis.

Figures 12 and 13 show the two crustal sections. Observed (black dots) inferred (dashed line), and computed (open circles) gravity values are shown above each of the models. Surface geologic contacts, lithologic intervals in wells, and seismic velocity intervals used to constrain the model are shown by contacts of density intervals with the surface, solid bars, and flattened H's, respectively.

Each of the sections consists of blocks of earth material assumed infinite in a direction perpendicular to the direction of the sections, which have average densities near 2.4 gm/cm^3. Variations in the densities and thicknesses of the near-surface layers result in computed gravity anomaly values in close agreement with observed and inferred free-air anomaly measurements. The densities used

Table 5. Approximate densities of lithologic intervals in wells and suggested correlations with velocity intervals from seismic reflection data.

Suggested correlation with seismic velocity interval	Total Thickness (meters)		Thickness of Constituent Lithologics (meters)		Estimated Density (gm/cm^3)	
	El Paso Nat. Gas	Sta-Tex Russel #1	El Paso Nat. Gas	Sta-Tex Russel #1	El Paso Nat. Gas	Sta-Tex Russel #1
I	91	820	Sediment 91	Sediment 820	1.90	2.10
II	674	445	Sediment 375 Basalt and Andesite 226 Rhyolite 73	Sediment 351 Basalt 94	2.41	2.38
III	699	52?	Sediment 699	Sediment 52?	2.25	2.25
IV	809		Sediment 436 Basalt and Andesite 58 Diorite and Gabbro 187 Rhyolite 128		2.59	

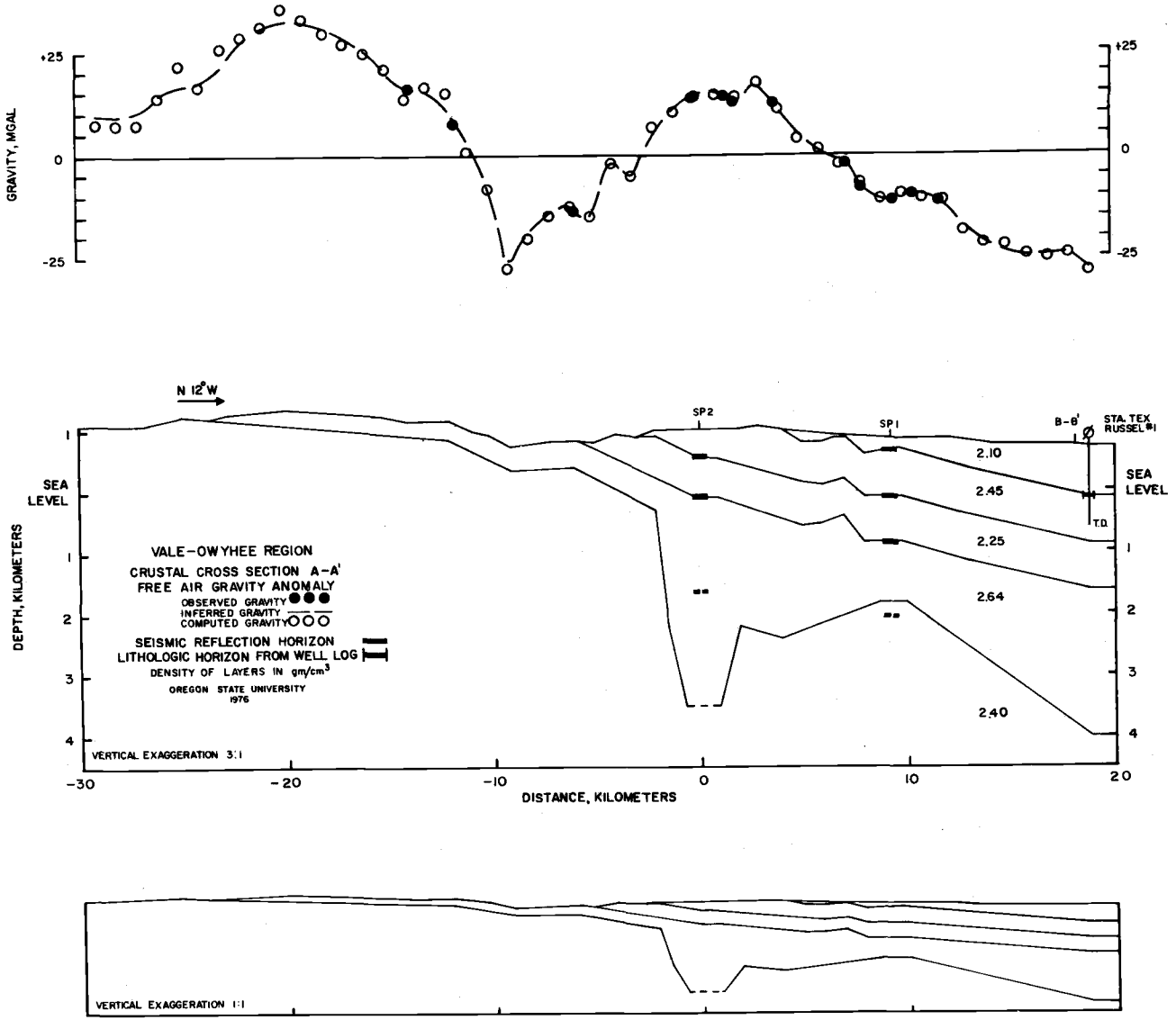

Figure 12. Crustal section A-A'.

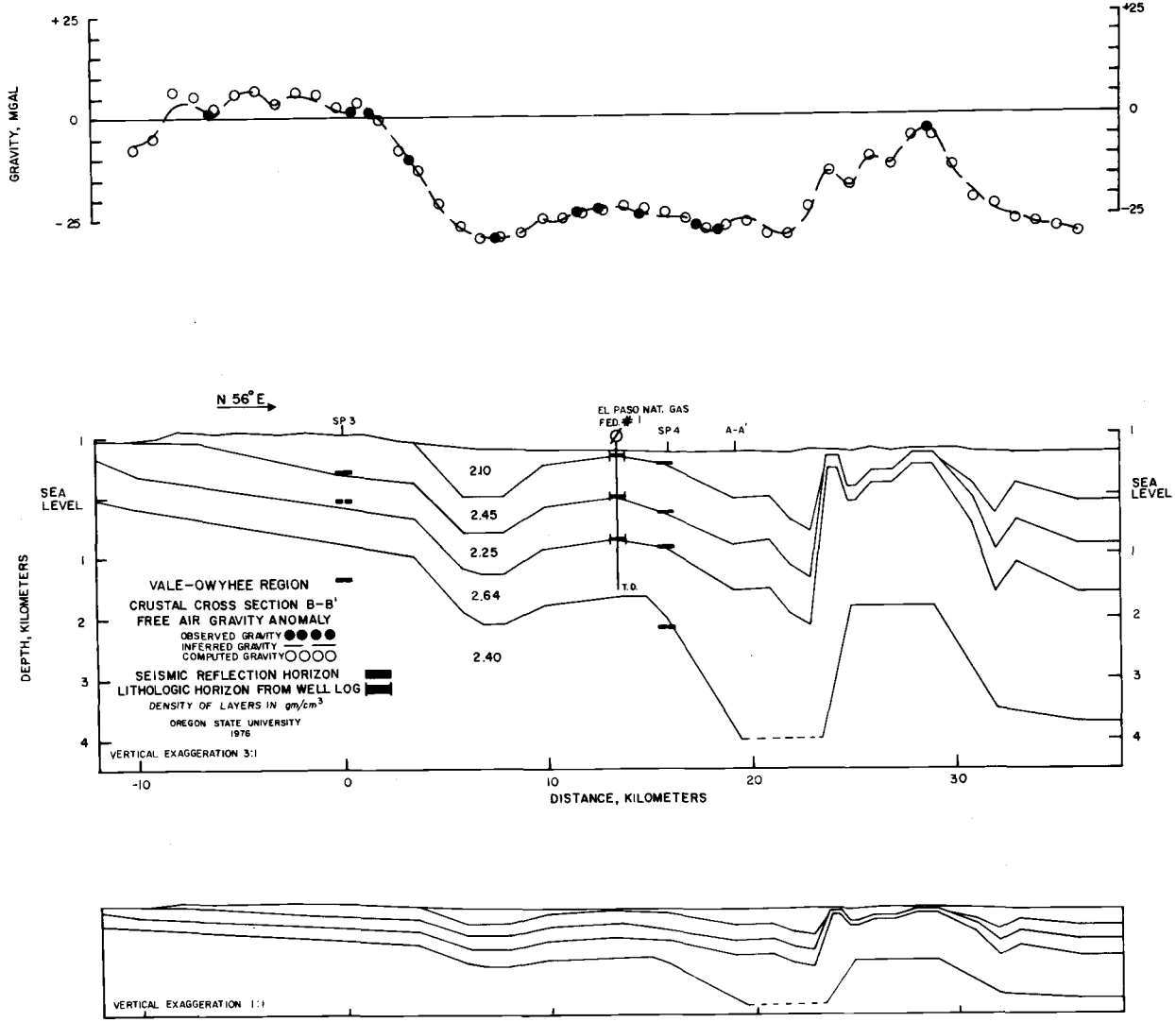

Figure 13. Crustal section B-B'.

for crustal layers are within the range of density values estimated for the seismic velocity intervals and lithologic intervals, as shown in Tables 4 and 5.

The dominant feature in section A-A' (figure 12) is a low northerly dip toward the axis of the Snake River Basin. The uppermost layer, with a density of 2.10 gm/cm^3, thickens toward the Snake River Basin. Surface outcrops and the Sta Tex well log show that this low density layer is predominantly sediments of the Chalk Butte Formation. The next two intervals, of densities 2.45 gm/cm^3 and 2.25 gm/cm^3, do not thicken toward the basin. Additionally, slight folding in these layers occurs just south of shot point 1. The well log and surface geologic data suggest that the upper, higher density block is predominantly basalts and interflow sediments of the Grassy Mountain Basalt, while beds of the Kern Basin and Deer Butte formations comprise the lower density interval.

A higher density block of 2.64 gm/cm^3 occurs below the three layers described above in the crustal model. Like the uppermost, low density block, this layer apparently thickens in a direction northward from shot point 1. Below shot point 2 an apparent thickening of this higher density material accounts for the high observed free-air anomaly. This apparent thickening can be interpreted as actual thickening of the stratigraphic sequence (e.g. by downwarping or faulting) or as an intrusion of high density material from below. Surface exposures and the El Paso Natural Gas well (projected onto section B-B') show that the upper part of this block is probably basic igneous rocks and sediments of the Owyhee Basalt. The lower part may be high density rhyolites from the top of the Sucker Creek Formation.

It is emphasized that wells used in this study are not deep enough to show the bottom of the high density block. Additionally, the bottom of the interval is too deep to be

resolved accurately by the seismic reflection technique employed. The bottom of the interval is therefore not as well constrained as contacts between other density intervals. Below the block of density 2.64 gm/cm^3, the model assumes an average crustal density of 2.40 gm/cm^3.

Crustal section B-B' (figure 13) shows the same density blocks used in section A-A'. Again, a shallow regional dip toward the axis of the Snake River Basin appears in the model. Thickening is proposed for the uppermost and lowermost layers of densities 2.10 and 2.64 gm/cm^3, respectively, while the other two blocks lack appreciable thickening toward the basin.

Two major structural features appear on the model. The El Paso Natural Gas well rests atop the Double Mountain Anticline, as mapped by Corcoran, et al. (1962). Five kilometers to the south a dacite core cuts the near surface sediments and basalt flows, as illustrated in the magnetic model of figure 6. The El Paso well does not show intrusive rocks until possibly very near the bottom of the well. The intrusive core of the Double Mountain Anticline in the area of section B-B' is therefore either lacking or too deep to be resolved by the gravity modeling. The model also shows that only the low density (2.10 gm/cm^3) layer thins above the anticline. This suggests that uplift occurred some time after deposition of the Grassy Mountain Basalt with an estimated density of 2.45 gm/cm^3.

The second major structural feature indicated by crustal model B-B' occurs between the 25 and 33 kilometer marks. This feature shows uplift and abrupt thinning of the 2.25 gm/cm^3 density block. The 2.45 gm/cm^3 layer laps up against the sides of the uplift and the whole structure is apparently buried by the upper, low density (2.10 gm/cm^3) block. The thickness of the high density (2.64 gm/cm^3) block remains fairly constant.

The Vale Buttes lie just north of crustal section B-B'. Corcoran, et al. (1962) mapped these as isolated outcrops of the Deer Butte Formation surrounded by the younger Chalk Butte Formation. Thus in the model the lower part of the 2.25 gm/cm^3 density layer correlates with the Deer Butte Formation.

A tectonic interpretation of the large structural feature on the east side of section B-B' suggests that sometime after deposition of the Owyhee Basalt (2.64 gm/cm^3) and the Deer Butte Formation (2.25 gm/cm^3) normal faulting occurred, leaving the feature in a high position as a horst. The relatively steep structural gradients on both sides of the feature are interpreted as the bounding faults of the horst. The structure remained as a topographic high and some of the Deer Butte Formation was eroded away. Further deposition then resulted in onlap of the Kern Basin Formation and Grassy Mountain Basalt against the sides of the high. The entire feature was then buried by deposition of the Chalk Butte Formation, except in a few places such as Vale Buttes.

As previously mentioned, Corcoran, et al. (1962) show several isolated outcrops of the Deer Butte Formation along a line trending south from Vale. These include Vale Buttes, Mitchell Butte, Deer Butte, and Pinnacle Point. All of these are located within the Bouguer anomaly high in the east-central part of the map of figure 6 discussed earlier. Thus, as suggested from section B-B', the gravity high may be due to high density (2.64 gm/cm^3) material brought near the surface as part of a horst. Steep gravity gradients on the edges of the high thus delineate buried north-south trending normal faults which dip away from the high.

As on the gravity maps, general trends on the second derivative map, shown in figure 11, are north-south south of latitude 44°00' North and northwest-southeast north of

44°00' North latitude. Second derivative highs generally correspond to Bouguer gravity highs and second derivative lows to Bouguer lows. It is interesting to note, however, that the second derivative map more closely resembles the free-air anomaly map than it resembles the complete Bouguer anomaly maps. In other words, it appears that the second derivative map shows high frequency trends due to topography as well as high frequency trends caused by deeper structures. There is a plausible explanation for this observation. High frequency gravity responses due to topography and seen plainly on the free-air gravity anomaly map of figure 5 are subdued, but not completely removed, by the Bouguer reduction technique. The second derivative method, however, will amplify short wavelength gravity anomalies relative to long wavelength anomalies. Because second derivatives were computed from complete Bouguer anomaly values it is believed that topographic effects still in the data contributed greatly to the resulting second derivatives. In areas of low relief, such as along the Gulf Coast, the second derivative of gravity has been shown to better outline subsurface features like salt domes (Dobrin, 1960). In the high relief Vale-Owyhee region, however, topography appears to contribute to second derivative anomalies as much as other types of short wavelength gravity effects. Therefore, the second derivative anomalies on figure 11 should be interpreted with caution, because it is difficult to distinguish effects due to subsurface structure or other phenomena from those due to topography.

One feature observed in the second derivative map (figure 11) which is not immediately apparent on the gravity maps (figures 5, 6 and 10) is the northeast-southwest trend observed in the area southwest of Vale, Oregon. This trend extends southwest from Vale to approximately latitude 43°40' North, longitude 117°35' West.

Hoover and Long (1975) show apparent resistivity anomalies which follow a similar trend in the area. These second derivative and resistivity trends, while not apparently related to topography or major structural features, may relate to the geothermal system of the Vale KGRA discussed below.

SUBSURFACE STRUCTURE OF THE VALE KGRA

Major Faulting and Folding

Figure 14 is a map of proposed major faults and folds in the vicinity of the Vale Known Geothermal Resource Area. The positions and relative movements on these features are based on the interpretation of data from this study and on previous works discussed below.

The proposed general structure includes four approximately north-south trending normal faults terminated on their northern ends by a northwest striking right-lateral strike-slip fault. Evidence for the existence of fault "A" comes from crustal sections A-A' and B-B' as well as the complete Bouguer anomaly maps of figures 6 and 10. On section B-B' the normal fault on the west side of the proposed horst shows an apparent dip to the southwest. Similarly, on section A-A' the steeply inclined feature to the south of shot point 2 can be interpreted as a normal fault with an apparent dip to the northwest. When these proposed faults are extrapolated to the surface and plotted on the complete Bouguer anomaly map (figure 6), they both lie in the area of steep gravity gradient on the west side of the Bouguer gravity high extending southward from Vale Buttes. The gravity high is interpreted as a horst. Thus a major normal fault (fault "A") dipping to the west may be inferred to follow the high gravity gradient on the west side of the proposed horst. Similarly, fault "B" is proposed to be a major normal fault which dips to the east and follows the north-south trending area of high gravity gradient on the east side of the horst. Proposed faults "A" and "B" also coincide with trends apparent on the telluric anomaly map (20 to 30 second period) of Hoover and Long (1975). Note that on the south side of section A-A' the proposed

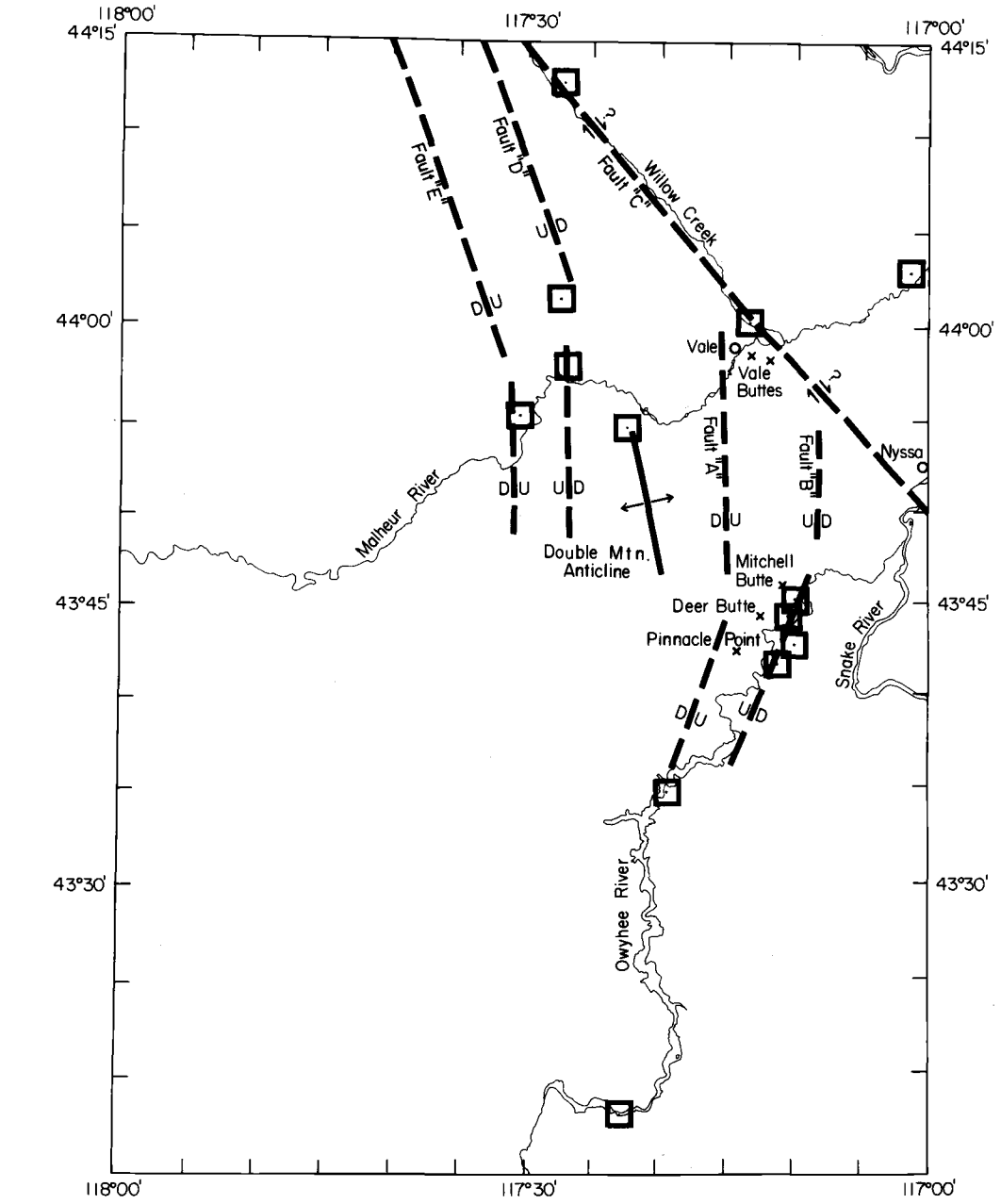

TECTONIC MAP

VALE-OWYHEE REGION, MALHEUR COUNTY, OREGON

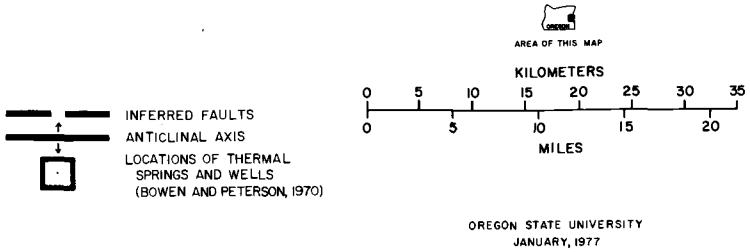

OREGON STATE UNIVERSITY
JANUARY, 1977

Figure 14. Tectonic map of the Vale-Owyhee region. Location of thermal springs and wells from Bowen and Peterson (1970).

horst has been eroded to the extent that the bottom part of the Owyhee Basalt (2.64 gm/cm^3) is exposed at the surface.

The bounding fault on the eastern side of the horst of crustal section B-B' lies in a northwest-southeast trending zone of high gravity gradient extending across the northeast part of the complete Bouguer anomaly map. Faults "A" and "B" both appear to terminate abruptly at this zone. Furthermore, other Bouguer anomaly trends, as well as surface geologic (Newton and Corcoran, 1963) trends, do not cross this zone in the mapped area.

Lawrence (1976) presents a possible explanation for the abrupt change in surface trends observed at Vale, based partly on an ERTS photo mosaic of the Pacific Northwest. He suggests east-west extension in the Basin and Range Province is accommodated for by four major zones of northwest-southeast trending strike-slip faults on the northern end of the province. The proposed movement on these faults is right-lateral. One of these faults appears as fault "C" on figure 14. As Lawrence suggests, the straight flow of Willow Creek is apparently due to the existence of this fault. He further shows that a portion of the Snake River in Idaho follows this lineation. Baldwin and Hill (1960) present a gravity study of an area of Idaho adjacent to the Vale-Owyhee region. They show that the steep gradients south of the gravity high which begins at latitude 43°55' North, longitude 117°00' West (near Nyssa, Oregon) may be traced in a southeasterly direction to a point well past Nampa, Idaho. Additionally, Hoover and Long (1975), from mapping of telluric anomalies of 20 to 30 second period, show a high anomaly gradient following the course of Willow Creek southeastward into Vale. Thus it is evident that the existence of this major structure is well documented, though relative motion of opposite sides of the feature is not immediately evident. The suggested right lateral motion of the fault is presumed by Lawrence (1976) to be quite

small (a few kilometers at most), since the area of extension in the Basin and Range Province south of Vale is quite narrow. If this is true, then some dip-slip movement apparently occurs along the fault, because it would take more than just a few kilometers of right-lateral movement to give the amount of vertical offset seen at the 30 kilometer mark on crustal section B-B' (figure 13).

The Willow Creek Fault of Bowen and Blackwell (1975) follows closely the course of fault "C" north of Vale. As they point out, a large Bouguer gravity low suggests that the zone to the west of Willow Creek has been down-dropped as a graben. This gravity low is very evident on the Bouguer anomaly maps of figures 6 and 10 and was discussed earlier in this paper. A component of normal (down-to-the-southwest) movement is therefore proposed for the portion of fault "C" following Willow Creek from fault "A" to the northern part of the map.

Fault "D" is proposed to lie in the area of high Bouguer gravity gradient on the western side of the proposed graben. North of the Malheur River this fault has the same down-to-the-northeast sense of motion as the Bully Creek fault proposed by Bowen and Blackwell (1975). The Bouguer anomaly map of figure 6, however, suggests that fault "D" follows more of a northerly trend than the proposed Bully Creek fault and that it probably terminates at fault "C" (Willow Creek fault) just off the northern edge of the map.

Bouguer anomaly trends suggest that another fault (fault "E") may parallel fault "D". This in turn suggests that the anomaly high between the proposed faults is another horst. The low gradient on the west side of the gravity high, however, suggests that the throw on proposed fault "E" is probably not nearly as great as the one to two kilometers suggested for the other proposed faults by crustal sections A-A' and B-B'.

Complete Bouguer gravity anomaly trends suggest that south of the Malheur River the trends of proposed faults "D" and "E" change to a more north-south direction. This may be due to actual bending or to a series of offsets of the fault surfaces. On crustal section B-B' the relatively steep dips shown between the three and six kilometer marks may actually show the zone where fault "D" crosses the crustal section. Fault "E" may either die out before it reaches the line of the crustal section or it may cross the section with too little throw to be resolved by gravity modeling.

Bending or offsets of the proposed faults may be due to the orientation of tectonic forces which have operated in the area. The region south of the Malheur River has probably been subjected to extension common to the Basin and Range Province (Lawrence, 1976). Scholz, et al. (1971) show that the extension direction for the province ranges from east-west to northwest-southeast. Thus the north-south trend of normal faults south of the Malheur River and the proposed right-lateral movement of fault "C" can be accounted for by east-west extension. North of the Malheur River effects of downwarp of the Snake River Basin probably tend to bend the direction of extension to a more northeast-southwest orientation. Thus horst and graben blocks between proposed faults "C", "D", and "E" on the northern part of the map strike N 20°W.

Bouguer gravity anomaly values become more positive toward the northeast corner of the mapped area. Anomaly trends in this area tend to follow the trend of the Snake River Basin, the axis of which lies just northeast of the mapped area. These high values suggest that the basin is filled with a greater amount of high density material (e.g. basalt) than areas on the rest of the map. A similar hypothesis is suggested by Baldwin and Hill (1960) for the adjacent area in Idaho. Their map shows Bouguer gravity

lows over the (granitic) Idaho Batholith and highs over the adjacent (basaltic) Snake River plain.

The El Paso Natural Gas, Federal #1 well lies within the graben between proposed faults "A" and "D". As previously discussed, this well rests upon the axis of the Double Mountain Anticline. Figure 14 shows the mapped anticline axis based on crustal section B-B', the El Paso well, and outcrops of igneous intrusives mapped by Corcoran, et al. (1962). The lack of thinning of formations older than the Chalk Butte Formation above the anticline suggests that uplift occurred after deposition of at least part of the Chalk Butte Formation. Furthermore, because intrusives at Double Mountain cut sediments of the Chalk Butte Formation, it is apparent that at least some (and maybe all) of the uplift occurred after deposition of the Chalk Butte Formation. The Chalk Butte Formation covers most of the proposed major faults in this study and there is no evidence that any of the faults cut the formation. The Double Mountain Anticline is therefore interpreted as a structural high formed by intrusion of igneous material between faults "A" and "D". This intrusion is believed to have occurred at the same time or after formation of the graben.

Relation of Structure to Thermal Activity

Roy, et al. (1971) show the Vale Known Geothermal Resource Area to lie within a broad area of the western United States having heat flow values greater than 2 Heat Flow Units (μcal cm^{-2} sec^{-1}). The average heat flow for continental areas is about 1.43 HFU (Garland, 1971). Several surface thermal springs and wells, discussed by Bowen and Peterson (1970), occur in the Vale area and are shown on the tectonic map of the Vale-Owyhee region (figure 14). Most of the thermal springs occur along proposed faults in the area. Four hot springs near the Owyhee

River are close to the proposed trace of fault "B". From north to south these are Mitchell Butte Hot Springs, Deer Butte Hot Springs, North Black Willow Spring, and South Black Willow Spring. Because the trend of these springs and the course of the Owyhee River in this area both follow the trend of a steep Bouguer gravity gradient shown in figure 6, it is suggested that both the geothermal activity and this portion of the course of the river are controlled by fault "B". A similar argument holds for proposed fault "C". Willow Creek follows the trend of high gravity gradient in the area. Two thermal springs are along the creek -- Vale Hot Springs near Vale and Jamieson Hot Spring northwest of Jamieson. Thermal manifestations along proposed fault "D" are Neal Hot Springs on Bully Creek and the Nelson Well on the Malheur River, which encountered thermal waters near the surface. An unnamed hot spring occurs on the Malheur River near fault "E". Additionally, an oil test well in Sand Hollow along the proposed axis of the Double Mountain Anticline penetrated thermal waters at a shallow depth. These relations suggest that surface manifestations of hydrothermal activity in the area are controlled by the proposed major structural features shown in figure 14.

Hoover and Long (1975) present an audio-magnetotelluric study of the Vale KGRA and adjacent areas to the northeast in Idaho. They show that the principal apparent resistivity trends in the Snake River Basin are northeast-southwest, similar to the complete Bouguer second derivative trends southwest of Vale, Oregon, mentioned above. Furthermore, a large resistivity low extends from the area of thermal activity around Vale to the area of Cane Creek hot springs northeast of Weiser, Idaho. They attribute this anomaly low to hot saline waters and alteration within the sedimentary section. They imply that since water circulation

is downdip or updip within the sedimentary section, resistivity trends are in an updip-downdip direction. Leakage of thermal waters to the surface, however, will probably be along faults, which do not necessarily show the same trends as the resistivity data. Hoover and Long point out a similar situation in the Suprise Valley, California, KGRA. Faults there are of the north-south Basin and Range type but trends related to the geothermal system are to the northwest.

Hose and Taylor (1974) present a discussion of geothermal systems in northern Nevada. They suggest that surface geothermal manifestations there result from circulation of waters along Basin and Range faults. These faults are delineated approximately by the steepest gradients of Bouguer gravity anomalies, as at Vale, and also in many cases by surface expressions such as mountain fronts. The model proposed by Hose and Taylor suggests that meteoric waters flow down along Basin and Range faults, becoming heated by the high geothermal gradient in the area. The hot waters, after some lateral flow through permeable layers, rise along other faults in the area. This model also seems applicable to the Vale KGRA, because thermal springs or near surface thermal waters apparently occur along faults marked by high gravity gradients or along other zones of weakness such as the axis of the Double Mountain Anticline.

CONCLUSIONS

A two-dimensional crustal model constrained by total field magnetic measurements shows that truncated edges of uplifted basalt flows can account for high frequency magnetic anomalies at Double Mountain, southwest of Vale, Oregon. Analysis of magnetic data shows that the depth to the magnetic anomaly source is at least 150 meters in an area of Cow Hollow covered by sediments of the Chalk Butte Formation, and less than 30 meters in areas where surface outcrops of the Grassy Mountain Basalt occur.

Seismic reflection data show estimated interval velocities from 1.9 to 3.4 km/sec, characteristic of sedimentary sequences, and higher velocity intervals, from 3.4 to 7.0 km/sec, suggestive of sequences of basalt and intercalated sediments. Calculated interval velocities and thicknesses correlate approximately with the stratigraphic sequence of Corcoran, et al. (1962) and lithologic descriptions of cuttings from nearby petroleum exploratory wells by Newton and Corcoran (1963). Two-dimensional crustal models south and southwest of Vale, constrained by geophysical and published geologic data, suggest a major structural feature, interpreted as a horst block, extending southward from Vale Buttes to the Owyhee Reservoir. High Bouguer gravity anomaly gradients, trending north-south south of Vale and northeast-southwest along the Owyhee River, delineate bounding faults on the horst.

Free-air and complete Bouguer gravity anomaly maps, and a map of the second derivative of gravity, show a high gravity gradient following the course of Willow Creek, northwest of Vale, and extending southeastward into Idaho. These anomalies occur along a topographic trend postulated by Lawrence (1976) as the surface expression of a major right-lateral strike-slip fault zone which terminates the

Basin and Range Province. High gravity anomaly gradients suggest two major faults bounding horst and graben blocks west and northwest of Vale. A proposed down-to-the-northeast normal fault strikes N 20°W north of the Bully Creek Reservoir and shows offset or bending to a north-south trend south of the reservoir. Paralleling this fault, approximately five kilometers to the west, is a proposed down-to-the-southwest normal fault.

Thermal springs and wells in the Vale-Owyhee region, mapped by Bowen and Peterson (1970), occur along or near proposed major faults in the area. This suggests that the faults serve as zones of high permeability for the flow of deep thermal waters to the surface.

BIBLIOGRAPHY

Adachi, R. 1954. Fundamental relations on the seismic prospecting. Kumamoto Journal of Science A(2):18-23.

Baldwin, H.L. and D.P. Hill. 1960. Gravity survey in part of the Snake River Plain, Idaho -- A preliminary report. U.S. Geological Survey, open file report (200) R290, No. 511.

Berg, J.W. and J.T. Thiruvathukal. 1965. Gravity base station network, Oregon. Journal of Geophysical Research 70:3325-3330.

Blakely, R.J. 1975. Unpublished computer program TWOMAG. Geophysics Group, School of Oceanography, Oregon State University, Corvallis.

Bowen, R.G. and N.V. Peterson. 1970. Thermal springs and wells in Oregon. Oregon Department of Geology and Mineral Industries, miscellaneous paper number 14.

Bowen, R.G. 1972. Geothermal gradient studies in Oregon. ORE BIN 34(4):68-71.

Bowen, R.G. and D.D. Blackwell. 1975. The Cow Hollow geothermal anomaly, Malheur County, Oregon. ORE BIN 37(7):109-121.

Bryan, K. 1929. Geology of reservoir and dam sites with a report on the Owyhee Irrigation project, Oregon. U.S. Geological Survey, water-supply paper 597-A:89 p.

Cope, E.D. 1883. On the fishes of the Recent and Pliocene lakes of the western part of the Great Basin, and of the Idaho Pliocene lake. Academy of the Natural Sciences of Philadelphia Proceedings:134-166.

Corcoran, R.E., R.A. Doak, P.W. Porter, F.I. Pritchett, and N.C. Privrasky. 1962. Geology of the Mitchell Butte Quadrangle, Oregon. State of Oregon Department of Geology and Mineral Industries, geological map series 2.

Couch, R., W. French, M. Gemperle, and A. Johnson. 1975. Geophysical measurements in the Vale, Oregon Geothermal Resource Area. ORE BIN 37(8):125-129.

Couch, R. and B. Baker. 1977. Geophysical investigations of the Vale-Owyhee Geothermal Region, Malheur County, Oregon. Technical Report No. 2. U.S. Geological Survey, Geothermal Research Program.

Dobrin, M.B. 1960. Introduction to geophysical prospecting. New York, McGraw-Hill. 446 p.

Garland, G.D. 1971. Introduction to geophysics. Philadelphia, W.B. Saunders Company. 420 p.

Gemperle, M. 1975. Two-dimensional gravity cross section computer program - source blocks and field points generalized, GRAV2DLD. Supplement to geophysical data reduction technical report, School of Oceanography, Oregon State University, Corvallis.

Godwin, L.W., L.B. Haigler, R.L. Rioux, D.E. White, L.J.P. Muffler, and R.G. Wayland. 1971. Classification of public lands valuable for geothermal steam and associated geothermal resources. U.S. Geological Survey, Circular 647. 18 p.

Grant, F.S. and G.F. West. 1965. Interpretation theory in applied geophysics. New York, McGraw-Hill. 584 p.

Henderson, R.G. and I. Zietz. 1949. The computation of second vertical derivatives of geomagnetic fields. Geophysics 14(4):508-516.

Hoover, D.B. and C.L. Long. 1975. Audio-magnetotelluric methods in reconnaisance geothermal exploration. U.S. Geological Survey, open file report 75-362. 25 p.

Hose, R.K. and B.E. Taylor. 1974. Geothermal systems of Northern Nevada. U.S. Geological Survey, open file report 74:271. 27 p.

Hull, D. 1975. Geothermal studies in the Vale area, Malheur County, Oregon. ORE BIN 37(6):104-106.

Kittleman, L.R., A.R. Green, A.R. Hagood, A.M. Johnson, J.M. McMurray, R.G. Russell, and D.A. Weeden. 1965. Cenozoic stratigraphy of the Owyhee region, southeastern Oregon. Museum of Natural History, University of Oregon, bulletin number 1. 45 p.

Kittleman, L.R., A.R. Green, G.H. Haddock, A.R. Hagood, A.M. Johnson, J.M. McMurray, R.G. Russell, and D.A. Weeden. 1967. Geologic map of the Owyhee region, Malheur County, Oregon. Museum of Natural History, University of Oregon, bulletin number 8.

Kittleman, L.R. 1973. Guide to the geology of the Owyhee region of Oregon. Museum of Natural History, University of Oregon, bulletin number 21. 61 p.

Larson, K. and R. Couch. 1975. Preliminary maps of the Vale area, Malheur County, Oregon. ORE BIN 37(8):138-142.

Lawrence, R.D. 1976. Strike-slip faulting terminates the Basin and Range province in Oregon. Geological Society of America Bulletin 87:846-850.

Ludwig, W.J., J.E. Nafe, and C.L. Drake. 1971. Seismic refraction. In: The Sea, Volume 4, Part I, ed. by Arthur E. Maxwell, New York, Wiley, p. 53-84.

Newton, V.C. and R.E. Corcoran. 1963. Petroleum geology of the western Snake River Basin, Oregon-Idaho. State of Oregon Department of Geology and Mineral Industries, oil and gas investigation number 1. 67 p.

Peters, L.J. 1949. The direct approach to magnetic interpretation and its practical applications. Geophysics 14(3):290-320.

Roy, R.F., D.D. Blackwell, and E.R. Decker. 1971. Continental heat flow. In: Nature of the Solid Earth, ed. by E.C. Robertson, New York, McGraw-Hill, p. 506-543.

Scholz, C.H., M. Barazangi, and M.L. Sbar. 1971. Late Cenozoic evolution of the Great Basin, western United States. Geological Society of American Bulletin 82:2979-2990.

Schouten, H. and K. McCamy. 1972. Filtering marine magnetic anomalies. Journal of Geophysical Research 77(35):7089-7099.

Talwani, M., J.L. Worzel, and M. Landisman. 1959. Rapid gravity computations for two-dimensional bodies with application to the Mendocino submarine fracture zone. Journal of Geophysical Research 64:49-59.

Talwani, M. and J.R. Heirtzler. 1964. Computation of magnetic anomalies caused by two-dimensional structures of arbitrary shape. In: Computers in the Mineral Industries. Stanford University Publications, Volume IX, number 1, p. 464-480.

Thiruvathukal, J.V., J.W. Berg, Jr. and D.F. Heinrichs. 1970. Regional gravity in Oregon. Geological Society of America Bulletin 81:725-738.

Van Orstrand, C.E. 1935. Temperatures in the lava beds of east-central and south-central Oregon. American Journal of Science 35(205).